Comparison of quantitative IRT to estimate U-value using different approximations of ECHTC in multi-leaf walls

1. Introduction

Climate change, the reduction of both carbon dioxide emissions and the energy consumption constitute some of the main concerns in today´s society. In this regard, the building sector plays a fundamental role. Approximately 40% of the total energy consumption from human activities is attributed to the building sector [1,2], generating 38% of greenhouse gas emissions [2]. This is due to the deficient behaviour of the envelope of the existing building stock, either by its age or by the fact that its energy behaviour has frequently been an underestimated aspect during the projection and execution phase [3,4]. In Spain, most of the building stock was built in the period corresponding to the second third of the 20th century [5]. That building period was characterised by not using insulation in its building solutions, causing that the limit values of energy loss through the envelope established by the Spanish Technical Building Code are overcome [5]. Therefore, the envelope of the existing buildings stock does not meet the newer needs of society, leading to important economic and environmental impacts. From the different components which constitute the envelope, the façade is where the buildings suffer greater energy losses [5], since it is the element of major area which is in contact with the external air. Due to this aspect, the energy demand reduction and the proposal of energy conservation measures (ECMs) are the most priority goals for the building sector [6].

From the different properties which define the energy behaviour of a building, the thermal transmittance (*U*-value) is one of the most important [7]. Its significance lies in the fact that most existing building stock has thermal transmittance values in façades which exceed the maximum admissible limits [5]. Furthermore, this circumstance is worsened by the progressive deterioration of façades due to the influence of environmental agents [8].

A correct estimation of *U*-value, along with other parameters such as the available budget, the thickness of the wall, etc. [9], will allow to define ECMs for façades, leading to the reduction of the HVAC systems consumption, the increase of number of thermal comfort hours, etc. To determine the *U*-value, there are different methods, both theoretical and experimental.

From the experimental methods, the method with a higher implementation is the heat flow meter method, which is included in the standard ISO9869-1 [10]. This method determines the *U*-value by measuring internal and external temperatures as well as the heat flow through the wall. It has been widely studied in several works, but it is related to operational and metrological problems which can distort results. In this sense, different studies [11,12] have shown that placing the heat flux meter in the wall can cause a perturbation in the heat flux, and consequently the results obtained can be no representative. The error associated with the heat flux measurement is the variable which most contribute to obtaining atypical results [13], with deviations up to 26% [14]. Despite these aspects, the need for guaranteeing stationary conditions during the performance of the test can lead to carry out long-term monitoring, even with a duration of 2 weeks [15,16].

Due to these difficulties, alternative methods to the heat flow meter method have arisen, such as the air–surface temperature ratio method, the simple hot box-heat flow meter method, and qualitative methods through infrared thermography. The air–surface temperature ratio method (also known as thermometric method) is an alternative to the heat flow meter method, since it determines the *U*-value of a wall through the measurement of the internal surface temperature of the element as well as of the environmental temperatures by using temperature probes [17]. The main difference of this method with respect to the heat flow meter method is that the error associated with the placing of probes is reduced, thus decreasing the maximum error of 26% of the heat flux plate up to 6% of the surface temperature probe [14]. This method behaves similarly to the heat flow meter method, since, in steady state conditions, differences lower than 5% can be obtained between the thermometric method and the heat flow meter method [18].

Meng et al. [19] developed the simple hot box-heat flow meter method as an implementation of classic hot-box methods in existing buildings. Hot-box methods consist of placing a study sampling between two rooms with a constant temperature difference [20], so the test is not limited by weather conditions [21]. The method developed by Meng et al. [19] is an extension of works carried out by several research groups on applying hot-box methods in existing walls. These previous works [22–24] developed the temperature control box-heat flow meter method by placing a hot-box at the internal surface of the wall, cooling or heating according to the time of year. The application of the method by Meng et al. [19] consisted of placing a simple hot box which only heats its internal volume. In addition, this box is placed at the surface of the wall in which the temperature is higher. Therefore, the placing of the box varies depending on the season (i.e. inside the room in winter and outside the room in summer). The use of this equipment allows to guarantee a steady temperature differential during the test. Variables of heat flux and temperatures are monitored by using probes employed in the previous methods. Despite these advantages, the installation of the hot box constitutes an aspect that could limit the use of this method in actual case studies.

In recent years, several methods determining the thermal transmittance through infrared thermography (IRT) have arisen so that there are different equations depending on whether tests are performed from the interior or the exterior.

External methods can be classified into two different models proposed by Albatici and Tonelli [25] and by Dall'O' et al. [26], using both models the same convective correlation. Firstly, Albatici and Tonelli [25] applied their method at three typologies of façades, and then these authors extended their study [27] by monitoring different types of walls throughout 3 years. These authors detected that the method was limited by environmental conditions. On the other hand, Dall'O' et al. [26] suggested an alternative formulation and applied their model in 14 case studies. Both methods were employed by Nardi et al. [28] obtaining similar results, although the test was carried out under controlled environmental conditions inside a hot box without wind. Thus, the usefulness of external methods should be studied in actual conditions. Regarding convective correlations, Evangelisti et al. [29] studied the formulation of the thermal transmittance from the exterior, using some convective correlations for special architectural geometries, such as balconies and porticos.

Both the method by Albatici and Tonelli [25] and the method by Dall'O' et al. [26] used the same convective correlation. However, in the scientific literature there is a wide variety of external convective heat transfer coefficient (ECHTC) depending on both the wind speed and dimensionless numbers on exterior surfaces. The use of these coefficients has not been analysed to assess the thermal transmittance. Hence, it is intended to fill the existing gap in the state of the art. A detailed analysis of tests performed from the exterior is carried out in this paper, studying different alternative equations for *U*-value depending on the different approaches existing in the literature for the external convective heat transfer coefficient (ECHTC). For this purpose, three multi-leaf walls from different building periods located in the Csa climate region were monitored.

2. Existing methods of *U*-value through IRT from the exterior of the wall

The thermal transmittance of a wall is given by the relationship between the heat flux through the wall (q) and the difference of the internal and external air temperatures $(T_i - T_e)$, according to the average method from ISO 9869-1:

$$U = \frac{q}{T_i - T_e} \quad (1)$$

The heat flux through the wall from Eq. (1) can be approximated to the sum of the heat flux by convection and radiation:

$$q = q_c + q_r \quad (2)$$

From Eq. (2), the heat flux by radiation can be expressed with the Stefan-Boltzmann Law as follows:

$$q_r = \sigma\, \mathcal{E} \left({T_w}^4 - {T_e}^4 \right) \quad (3)$$

Where σ [W/(m^{2}K^4)] is the Stefan-Boltzmann constant ($5.67 \cdot 10^{-8}$), $\mathcal{E}$ [dimensionless] is the emissivity of the wall, and T_w [K] is the surface temperature of the wall.

The heat flux by convection can be expressed by the Newton's Law of Convective Cooling:

$$q_c = h_e \Delta T_{we} \quad (4)$$

Where h_e [W/(m^{2}K)] is the ECHTC, and ΔT_{we} [K] is the temperature difference between T_w and T_e.

From the combination of Eqs. (1) - (4), a new expression can be obtained to have the thermal transmittance of a wall. In that new expression, the mechanism of conduction is not considered since the controlling factor is the ECHTC:

$$U = \frac{h_e\, \Delta T_{we} + \sigma\, \mathcal{E} \left({T_w}^4 - {T_e}^4 \right)}{T_i - T_e} \quad (5)$$

By means of Eq. (5), methods of Albatici and Tonelli [25] and of Dall'O' et al. [26] were suggested. The first of them used Jürges correlation ($5.8 + 3.8054v$), documented by Watanabe [30], for the ECHTC. Moreover, since tests were carried out when the local wind speed is low (< 1 m/s), Albatici and Tonelli took the decision of simplifying that correlation by removing the constant term with the aim of avoiding the predominance of the convection transfer over the radiation, obtaining the following equation:

$$U = \frac{3.8054\, v\, \Delta T_{we} + \sigma\, \mathcal{E} \left({T_w}^4 - {T_e}^4 \right)}{T_i - T_e} \quad (6)$$

Where v [m/s] is the local wind speed.

On the other hand, Dall'O' et al. [26] only took into account the contribution of the heat transfer by convection and these authors did not simplified the convective correlation of Jürges:

$$U = \frac{(5.8 + 3.8054\, v)\, \Delta T_{we}}{T_i - T_e} \quad (7)$$

As mentioned above, methods need very specific environmental conditions to be correctly applied. To ensure stationary conditions, it is necessary to secure a thermal gradient higher than 10 °C as well as a stable heat transfer during at least 3 h before the measurement [25,27]. Other environmental aspects that should be guaranteed during the performance of the test are [25,27,31,32]: (i) wind speed should be between 0.1 and 1 m/s; (ii) the element under study should not be exposed to radiation sources; and (iii) there should be no rainfalls. Guaranteeing these environmental conditions allows to secure the representation of the obtained results.

3. ECHTC correlations

Jürges correlation, published by Watanabe, is not the only one. In scientific literature, there is a huge variety of correlations of experimental data for vertical surfaces. These correlations are generated as correlations depending on wind speed values or depending on the use of dimensionless numbers, such as the Nusselt number or the Reynolds number.

In the next sub-sections, a detailed summary of the different ECHTCs used to obtain thermal transmittance results by means of the measured data is included.

3.1. ECHTC correlations depending on the wind speed

The set of Jürges equations is based on adjustments in the ECHTC for a heated copper square plate in a wind tunnel measurement (WTM) [33]. However, Cole and Sturrock [34] pointed out several problems concerning results of wind tunnel experiments, so the ECHTC measured in a small flat plate showed disadvantages by applying the ECHTC to big building surfaces [33]. On the other hand, Watmuff et al. [35] said that the convective correlation indicated by Jürges has a radiation component, so its use in the formulation proposed by Albatici and Tonelli (Eq. (6)) can increase even more the predominance of the radiation component. Moreover, the relationship between the ECHTC and the wind speed depends on the position of the measurement and the size of the wall [33]. In this sense, the ECHTC in the corner of the building is higher than the one near the middle [33].

For this reason, the use of a unique correlation depending on the wind speed for the ECHTC can cause difficulties (e.g. the height of the wall, the closeness to corners, etc.) to be applied in different case studies. In the scientific literature, there are many expressions of correlation, some of them compiled by different authors [33,36,37]. When analysing these research, some aspects should be taken into account when comparing equations of correlation. On the one hand, the height of the wind speed is different depending on the research (roof wind speed, local wind speed, free stream wind speed, etc.). On the other hand, the perpendicular distance of separation to which the wind is measured with respect to the vertical surfaces is not often indicated. Due to this, it is quite difficult to apply the equations used in these experiments, since a wind flow pattern around a building considerably fluctuates, which means that the wind profile is highly dependent on the distance from the building envelope.

Table 1 includes a list of the different ECHTC correlations depending on the local wind speed which are used in this study. This local wind speed was used as it allows to determine the thermophysical behaviour of the envelope more precisely than other wind speeds, such as the free stream wind speed [29].

Table 1
Approximations of ECHTC correlations of the wind speed.

3.2. ECHTC correlations depending on dimensionless numbers

There are other correlations for the natural convection on a vertical plate at uniform temperature in which Nusselt, Raylegh or Reynolds dimensionless numbers are used. Their use in the field of the energy efficiency of buildings has been quite limited because of their difficulties of implementation [64].

However, a new research tried to apply the dimensionless approach to the thermal transmittance. Tejedor et al. [65] developed an equation of *U*-value to perform the IRT test from the interior, by using the Nusselt number proposed by Churchill and Chu [66] (Eq. (53)). This equation is valid for laminar and turbulent regime alike (Eq. (54)).

$$Nu_L = \left\{0.825 + \frac{0.387 Ra_L^{1/6}}{\left[1 + (0.492/Pr)^{9/16}\right]^{8/27}}\right\}^2 \tag{53}$$

$$U = \frac{\frac{k\left\{0.825 + \frac{0.387 Ra_L^{1/6}}{\left[1 + (0.492/Pr)^{9/16}\right]^{8/27}}\right\}^2}{L}(T_i - T_w) + \sigma\, \varepsilon \left(T_r^{\,4} - T_w^{\,4}\right)}{T_i - T_e} \tag{54}$$

Where Nu_L is the Nusselt number [dimensionless], Ra_L is the Rayleigh number [dimensionless], Pr is the Prandtl number [dimensionless], k is the thermal conductivity of the air [W/(mK)], L is the height of the wall [m], and T_r [K] is the reflected temperature.

The same approach from Eq. (54) can be proposed from the exterior, so the equation by Tejedor et al. [65] is adapted to external conditions:

$$U = \frac{\frac{k\left\{0.825 + \frac{0.387 Ra_L^{1/6}}{\left[1 + (0.492/Pr)^{9/16}\right]^{8/27}}\right\}^2}{L}\Delta T_{we} + \sigma\, \varepsilon \left(T_w^{\,4} - T_e^{\,4}\right)}{T_i - T_e} \tag{55}$$

Moreover, there is a huge variety of approximations of ECHTC using correlations of dimensionless numbers. Table 2 includes those correlations selected for this study due to their suitability for the kind of element required to be analysed.

Table 2
Approximations of ECHTC correlations of dimensionless numbers.

4. Methodology and experimental campaign

The experimental campaign consisted of monitoring three multi-leaf walls facing north. Buildings belong to the most representative building periods in Spain (see Table 3): (i) previous to the NBE-CT-79 (case study A); (ii) between the NBE-CT-79 and the RD 314/2006 (case study B); and (iii) posterior to RD 314/2006 (case study C).

Table 3
Technical characteristics and thermo-physical properties of case studies.

In each wall, a total of 4 different tests were performed. Conditions of the performance of tests were in adherence to the standard EN 13187. Tests were carried out with low wind speeds and avoiding rainfalls 48 h before their beginning [65,67]. Moreover, tests were planned to be performed those days in which the lowest external temperature was forecast, since this aspect, along with the use of heating equipment, allowed to guarantee a temperature difference of 10–15 °C between the interior and the exterior. Likewise, tests were carried out among those hours before and after the sunrise to guarantee an optimal temperature differential without fluctuations [65]. Each test lasted 2 hours and 50 minutes. The acquisition time step 15 s for temperatures and 1 s for the wind speed. Before beginning tests, the emissivity of walls was determined by using an adhesive tape with known emissivity, according to the ASTM E1933-14. It was only determined at the beginning of each test, since it is a fixed value which does not show variations due to environmental temperature oscillations [68].

The experimental campaign was carried out with equipment indicated in Table 4. All probes were placed at a height of 1.5 m from the floor. External air temperature sensors were placed as aligned as possible from the internal air temperature sensor, with a distance of 20 cm from the external side of the wall [14]. The hot-wire anemometer was placed with a perpendicular space of 10 cm from the wall [27,28]. Following Tejedor et al. [65], the thermography camera was placed 1.5 m away from the façade, with an inclination angle of 20°.

Table 4
Main technical specifications of the equipment employed.

The post-processing and data analysis were carried out using the FLIR Tools software and the R statistical programming language. Regarding the post-processing and analysis, it is important to highlight the following aspects: (i) the used wind speed was the average of instantaneous measurements during the test, according to recommendations given by some authors [25,26]; (ii) for the dimensionless approaches, the work fluid is the air, and values of viscosity and of thermal conductivity of the air as well as the Prandtl number were determined by means of a technical manual [69], depending on the external temperature in each test; (iii) the average value of thermal transmittance is obtained from the arithmetic mean of instantaneous measurements; and (iv) the uncertainty was determined by means of the combined standard uncertainty.

To determine the representation of the obtained values of the thermal transmittance, the method proposed in ISO 9869-1 was used, considering valid those results that showed a difference lower than 20%. However, for this study, the value from ISO 6946 was not used as reference value, but those values obtained with the heat flow meter method. Thus, values obtained by IRT methods were compared with those values obtained by the heat flow meter method, and results presenting a difference lower than 20% were considered representative. Results of the heat flow meter method were obtained from an experimental campaign on walls, which was carried out before tests of this study. Measurements were performed by using a heat flux plate FQA018C with the following characteristics: (i) dimensions of 120x120x1.5 mm; (ii) substrate of epoxy resin; (iii) range of ±2000 W/m^2; and (iv) accuracy of ±5%. In addition, thermocouples indicated in Table 4 were used to measure internal and external temperatures. Fig. 1 shows those values measured for each variable as well as the average thermal transmittance value obtained.

Fig. 1. Heat flux measurements (green line), external temperature (blue line) and internal temperature (red line), and average thermal transmittance (black line) for each case study.

5. Results and discussion

Firstly, it was important to analyse those variables measured in the different tests of the experimental campaign. In spite of having difficulties in obtaining temperature records with a difference higher than 10 °C in the Mediterranean climate region [17], tests were conducted when low temperatures were forecast. Consequently, this aspect guaranteed an adequate thermal gradient during tests. As can be seen in Figs. (2) – (4), the difference of external and internal temperature values measured during tests presented differences higher than 10 °C, and that difference was steady in each test. The local wind speed measured during tests was characterized by constant fluctuations around its mean value due to gusts of wind.

Fig. 2. Variables measured in test 4 of case study A: the internal air temperature (red), the external air temperature (blue), the external surface temperature (purple), and the wind speed (green).

Fig. 3. Variables measured in test 4 of case study B. Same colour codification as in Fig. 2.

Fig. 4. Variables measured in test 4 of case study C. Same colour codification as in Fig. 2.

Given different theoretical approaches are used in the existing research to determine the *U*-value from the exterior, the existing relationship between approaches was firstly determined. As seen above, the formulation can vary among three approaches: (i) only the convective heat transfer coefficient is used; (ii) the convective and radiative heat transfer coefficient is used; and (iii) convective and radiative heat transfer coefficient is used but simplifying the convective correlation by rejecting the constant term. For this reason, different approaches were applied by using all ECHTCs previously indicated (Eqs. (8) – (52)) in order to establish an adjustment degree and deviations presented by results through linear regressions among the different results. To do this, the linear correlation coefficient (R^2) (see Eq. (65)) and the mean absolute error (*MAE*) (see Eq. (66)) were determined as statistical parameters indicators of the adjustment degree.

$$R^2 = \frac{\sum_{i=1}^{n} (y_i - x_i)^2}{\sum_{i=1}^{n} x_i^2} \tag{65}$$

$$MAE = \frac{\sum_{i=1}^{n} |y_i - x_i|}{n} \tag{66}$$

Where n is the total number of dataset instances analysed, and x_i and y_i are the values assigned to the variables x and y at the instance i, respectively.

As can be seen in Fig. 5, point clouds of the different approaches presented a linear tendency between them. In this sense, those approaches which presented a lower correlation were the approach of convention with the approach of simplified convection and radiation, with a R^2 of 0.66 (see Table 5). On the other hand, the other two comparisons had a higher adjustment degree, with R^2 equal or higher than 0.85. Despite these existing correlations due to the linear tendencies presented by distributions of point clouds, great differences have been detected among those thermal transmittance values obtained by the different approaches. In this context, the *MAE* between the approach of convection and the approach of simplified convection and radiation was the lowest, since thermal transmittance values obtained by both approaches were not so high in comparison with those values from the approach of convection and radiation. Thus, high values associated with the approach of convection and radiation led to obtaining *MAEs* of 0.97 with respect to the approach of convection, and of 1.18 with respect to the approach of simplified convection and radiation. According to this analysis, great differences among the different approaches could be possible, so it is necessary to analyse the results obtained by using each theoretical approach.

Table 5
Statistical parameters of regressions of the different theoretical approaches.

Fig. 5. Point clouds of the different assumptions of formulation.

Before making the comparative study among equations, a cluster analysis was carried out to determine possible groups among ECHTCs as their equations are similar. So, this cluster analysis eases the analysis and discussion of results. To do this, the Ward method was used because it allows to generate small clusters. The value of the heat flux by convection was obtained for each ECHTC (Eq. (4)) in tests conducted in 3 case studies, and then the results obtained were used to establish the clusters. Based on the Euclidean distance (see Eq. (67)) it was determined that, for k=20 clusters, the most adequate approximation was obtained for ECHTC equations of the wind speed (see Fig. 6) and for k=6 clusters the most adequate approximation was obtained for ECHTC equations of dimensionless numbers (see Fig. 7). It is important to highlight that ECHTCs making restrictions regarding the type of surface finish were included in some of these clusters. Therefore, for these equations it is not necessary to make a distinction of the type of surface finish in order to apply them. In this sense, the following groups can be highlighted: clusters of Eqs. (15), (17) and (47) and of Eqs. (12) and (52), in which ECHTCs were grouped for rough and soft surfaces. Furthermore, differences were not detected among ECHTCs that restrict the direction of wind incidence (windward-leeward), obtaining grouped results for correlations of Liu and Harris (Eqs. (50) and (51)) and correlations of Yazdanian and Klems (Eqs. (34) and (35)). Likewise, the simplified convective correlation of Watanabe from the equation of Albatici and Tonelli (Eq. (6)) was grouped with Eqs. (26), (34) and (35), since these equations are exponential or linear without including a constant term in the straight regression line. For ECHTCs depending on dimensionless numbers, three different groups were obtained: (i) cluster a, with correlations of Nusselt and Jürges (Eq. (56)) and of Davies (Eq. (63)); (ii) cluster c, with correlations of Jürges (Eq. (59)) and of McAdams (Eqs. (60) and (61)); and (iii) cluster e, with correlations of Nusselt and Jürges (Eq. (57)) and of Jürges (Eq. (58)). The remaining equations were grouped in individual clusters.

$$d(x_i, x_j) = \left[\sum_{r=1}^{p} (x_{ir} - x_{jr})^2\right]^{1/2} \tag{67}$$

Where p is the number of variables, and x_i and x_j are two certain instances.

Fig. 6. Clustering dendrogram of ECHTC correlations depending on the wind speed.

Fig. 7. Clustering dendrogram of ECHTC correlations depending on dimensionless numbers.

After grouping the different equations, thermal transmittance results were obtained from the experimental campaign for the different tests. Firstly, results obtained for ECHTCs depending on wind speed values were analysed. For the approach of convection, there was a large disparity in the results obtained for the different clusters (see Table 6). In general terms, an ECHTC was not more adequate than the other. Furthermore, there were differences among tests of a same case study. For tests of case study A, a great variety of equations with representative results was only obtained in test 4. In the remaining tests of that case study, only clusters n, p and q, which belong to ECHTCs of Ito (Eq. (24)), of Cole and Sturrock (Eq. (25)), and of Jennings (Eq. (19)) respectively, obtained valid results. For the other two case studies, representative results were obtained for the different clusters, although none of them obtained valid results for all tests. Cluster j was the one which obtained a larger number of tests with valid results. However, in spite of being the cluster with a larger number of representative results, it is also important to highlight the good performance of clusters i and k, with 5 tests with representative results, and at least one of them was of each case study. On the other hand, cluster e which belongs to the equation of Dall'O' et al. (Eq. (7)) obtained valid results only in test 4 of case study A.

Table 6
Thermal transmittance results obtained for ECHTC correlations depending on the wind speed for the approach which only uses the convective heat transfer coefficient.

The approach of convection and radiation allowed to obtain different results in each test. In general terms, the incorporation of the radiative component increased the thermal transmittance value, reducing the number of representative results for all clusters. Results showed that the number of clusters with valid results was high in only two tests of case study A, whereas in the other two case studies valid results were obtained in 3 clusters of test 1 of case study B. In this sense, only cluster t obtained valid results in both case studies. Moreover, it is important to highlight that the correlation of Watmuff et al. (Eq. (27)), included in cluster j, obtained valid results in the approach of convection, whereas valid results were not obtained in the approach of convection and radiation. It is important to highlight that this convective correlation corrected the radiative contribution in which formulations of convection proposed by Jürges were included (one of them was used by Albatici and Tonelli (Eq. (6)) and by Dall'O' et al. (Eq. (7))). Another important aspect is the percentage contribution of convective and radiative components in each cluster. Fig. 8. represents percentage contributions of convective and radiative components in the different clusters for each case study. The incorporation of the radiative component presented a similar behaviour for each cluster in the 3 case studies, although the value of percentages had small variations. Thus, those clusters which presented a lower percentage of radiative heat flux on the total heat flux were clusters n, p and q (lower than 35%), whereas those clusters which had a greater influence were clusters r, s and t (higher than 70%). This last cluster belongs to convective correlations without a constant term in the straight regression line, which generates a lower convective coefficient in low wind speed. In this sense, as can be seen in Table 7, ECHTCs of cluster s, which establish limitations to be used for low wind speed (see Table 1), obtained similar results to the equation of Albatici and Tonelli, which is grouped in cluster t, with an average percentage deviation of 8.59%.

Table 7
Thermal transmittance results obtained for ECHTC correlations depending on the wind speed for the approach which uses the convective and radiative component.

Fig. 8. Percentage contributions of convective and radiative fluxes in the total heat flux for the approach of convection and radiation using ECHTC correlations depending on the wind speed.

To obtain thermal transmittance results through the application of convective correlations with the simplified approach, the group done with the cluster analysis was not used due to modifications presented by convective coefficients obtained for each equation. Thus, the individual analysis of each equation was carried out. As can be seen in Fig. 9, equations had a similar behaviour in most case studies, with small variations in some tests. For instance, in test 4 of case study A, a standard deviation of 0.12 W/(m^{2}K) was obtained, or in test 3 of case study B, with a standard deviation of 0.07 W/(m^{2}K), whereas in the remaining tests, standard deviations lower than 0.05 W/(m^{2}K) were obtained. These differences were due to the fact that the obtained average speeds were higher than the other tests, generating a greater difference among convective coefficients of the different equations. Hence, for the approach of simplified convection and radiation is indifferent to use the correlation of Watanabe (or some others analysed in this study) for very low wind speeds (as mentioned above, this is a requirement recommended by several authors [25–27]), since the main contribution of the simplified approach was due to the radiation. In this sense, the simplification of the convective correlation generated that the contribution of the radiative component was always higher than 75%, reaching 95% in some equations (see Fig. 10). Furthermore, valid results were only obtained in two tests: one belongs to case study A, and the other one belongs to case study B.

Fig. 9. Thermal transmittance results obtained for ECHTC correlations of the wind speed for the approach which uses the simplified convective component and the radiative component. Grey continuous line represents the thermal transmittance

value obtained by the heat flow meter method, and discontinuous line represents the maximum admissible deviation (20%) with respect to that value.

Fig. 10. Percentage contributions of convective and radiative fluxes in the total heat flux for the approach of simplified convection and radiation for ECHTC correlations depending on the wind speed.

Thus, results did not allow to establish an adequate ECHTC or approach for formulations of thermal transmittance measured from the exterior by using wind speed values, although it is possible to guarantee the suitability of using some ECHTCs: (i) for the approach of convection, equations of Watmuff et al. (Eq. (27)), Lunde (Eq. (30)), ISO 6946 (Eq. (45)), and of Liu and Harris (Eqs. (50) and (51)) obtained a huge number of representative results in the three kind of walls analysed; (ii) for the approach of convection and radiation, clusters a, b, c, e, f, g, h, k, l and o obtained valid results in the wall without insulation, while the use of clusters r, s and t obtained valid results in walls with insulation; and (iii) the use of the approach of simplified convection and radiation did not present great variations among the different types of equations for low wind speeds, obtaining valid results in walls without insulation or with insulation of small thickness.

With respect to ECHTC correlations depending on dimensionless numbers, different results were obtained for approaches of convection, as well as for approaches of convection and radiation. Table 8 indicates those thermal transmittance values obtained for the approach of convection. As can be seen, the approach of convection did not obtain valid results for none of clusters because results presented differences higher than 20% with respect to the value obtained with the heat flow meter method. This is due to the low convective coefficient obtained through these correlations. As can be seen in Fig. 11, the use of the combined approach of convection and radiation generated that the contribution of the radiative component was higher than 70% in all clusters, having percentages similar to the approach of simplified convection and radiation. Regarding thermal transmittance results obtained for the approach of convection and radiation, valid results were obtained for almost all clusters in two tests (see Table 9), although atypical results were obtained in the remaining tests.

Table 8
Thermal transmittance results obtained for ECHTC correlations of dimensionless numbers for the approach which only uses the convective component.

Fig. 11. Percentage contributions of convective and radiative fluxes in the total heat flux for the approach of convection and radiation using ECHTC correlations of dimensionless numbers.

Table 9
Thermal transmittance results obtained for ECHTC correlations of dimensionless numbers for the approach which uses the convective and radiative component.

Another aspect to highlight is that using the average wind speed instead of the measured instantaneous value caused a variation in formulations of thermal transmittance. As can be seen in Fig. 12, there were variations depending on the type of data used. For the approach of convection, the use of the measured instantaneous speed modified thermal transmittance results, consequently obtaining different numbers of clusters with representative results. In total, 31 valid results were obtained among the different tests using the average speed with respect to those 33 using the measured instantaneous speed at each instant. Furthermore, variations presented by results varied from one test to another, since they depend on oscillations that the wind speed had in each test, with variations in the thermal transmittance value reaching 67% in some clusters. In this sense, the greater differences in the number of clusters with valid results were in tests with greater oscillations in the wind speed, as in test 4 of case study A. Regarding the approach of convection and radiation, Fig. 12 shows a similar tendency to the approach of convection, with variations in the number of representative clusters (26 using the average speed, and 32 using the instantaneous speed at each instant), although most changes were in tests of case study A. Despite these differences, it was not possible to determine which type of wind speed had better features. Thus, further studies should determine those limitations of using the average speed and the measured instantaneous speed in different case studies.

Fig. 12. Variations of thermal transmittance results depending on the wind speed value used. Grey continuous line represents the estimated value of thermal transmittance, and discontinuous line represents the maximum admissible deviation (20%) with respect to that value.

6. Conclusions

In this paper, a comparative study of expressions of thermal transmittance by means of different external convective heat transfer coefficients for the quantitative method through infrared thermography has been conducted. In total, 46 correlations depending on the wind speed were analysed, as well as 9 correlations depending on dimensionless numbers. For this purpose, 3 walls belonging to different building periods were monitored in an experimental campaign. Based on the results obtained, the following conclusions can be established:

- Different approaches of formulation for determining the thermal transmittance presented a linear tendency among their point clouds, and there were great differences between the approach of convection and radiation and the other two approaches. In this sense, mean absolute errors of 0.97 were obtained with respect to the approach of convection, and of 1.18 with respect to the approach of the simplified convection and radiation.
- Clustering external convective heat transfer coefficients allowed to group equations limited by the type of surface finish (smooth-rough) or wind direction (windward-leeward). Moreover, the equation of Albatici and Tonelli was grouped with correlations of Cole and Sturrock [34] and of Yazdanian and Klems [54], since these correlations are exponential and linear correlations without including a constant term in their straight regression line. For correlations depending on dimensionless numbers, 3 clusters with different equations were obtained, and the remaining equations were in individual clusters.
- The different theoretical approaches of thermal transmittance for external convective heat transfer coefficients depending on the wind speed obtained different results for each cluster and each test. Given these differences, it was not possible to establish a more adequate external convective heat transfer coefficient or approach, although the suitability of using some of the external convective heat transfer coefficients was established: (i) for the approach of convection, equations of Watmuff et al. (Eq. (27)), of Lunde (Eq. (30)), of ISO 6946 (Eq. (45)), and of Liu and Harris (Eqs. (50) and (51)) obtained valid results in the three types of walls analysed; (ii) for the approach of convection, equations belonging to clusters a, b, c, e, f, g, h, k, l and o obtained valid results in the wall without insulation, whereas the use of equations of clusters r, s and t obtained valid results in walls with insulation; and (iii) for the approach of simplified convection and radiation, valid results were obtained in walls without insulation or with insulation of small thickness. In addition, similar results were obtained among the different equations of external convective heat transfer coefficient due to the wind speed when the speed was low.
- The percentage of contribution of the radiative component for each cluster varies from one case study to another, although there was a similar behaviour in each test, and clusters r, s and t (Eqs. (6), (9), (10), (11), (13), (14), (16), (21), (26), (34) and (35)) presented a greater influence of the radiative component, and n, p and q (Eqs. (19), (24) and (25)) presented a lower influence.
- From the dimensionless approaches, none of the external convective heat transfer coefficients analysed obtained representative results for the approach of convection, whereas the approach of convection and radiation allowed to obtain representative results in two tests, with a behaviour similar to the simplified approach of Albatici and Tonelli.
- The use of the average wind speed or a wind speed measured at each instant as input in the calculation procedure significantly modified thermal transmittance results obtained in each test. A greater variation was obtained in results of those tests in which the deviation presented by the instantaneous wind speed was high with respect to the mean value.

To conclude, the importance of this study is based on the lack of research analysing a huge number of correlations of external convective heat transfer coefficient depending on both the wind speed and dimensionless numbers. Further steps of this research will be focused on the analysis of internal convective heat transfer coefficients for methods of thermal transmittance.

References

[1] L. Pérez-Lombard, J. Ortiz, C. Pout, A review on buildings energy consumption information, Energy Build. 40 (2008) 394–398. doi:10.1016/j.enbuild.2007.03.007.

[2] United Nations Environment Programme, Building Design and Construction: Forging Resource Efficiency and Sustainable Development, Sustain. Build. Clim. Initiat. (2012).

[3] M. Dowson, A. Poole, D. Harrison, G. Susman, Domestic UK retrofit challenge: Barriers, incentives and current performance leading into the Green Deal, Energy Policy. 50 (2012) 294–305. doi:10.1016/j.enpol.2012.07.019.

[4] G. Stevens, J. Bradford, Do U-value insulation? England's field trial of solid wall insulation, Eceee 2013 Summer Study. (2013)

1269–1280.

[5] F. Kurtz, M. Monzón, B. López-Mesa, Energy and acoustics related obsolescence of social housing of Spain's post-war in less favoured urban areas. The case of Zaragoza, Inf. La Construcción. 67 (2015) m021. doi:10.3989/ic.14.062.

[6] M. Gangolells, M. Casals, N. Forcada, M. MacArulla, E. Cuerva, Energy mapping of existing building stock in Spain, J. Clean. Prod. 112 (2016) 3895–3904. doi:10.1016/j.jclepro.2015.05.105.

[7] S. Ferrari, V. Zanotto, The thermal performance of walls under actual service conditions: Evaluating the results of climatic chamber tests, Constr. Build. Mater. 43 (2013) 309–316. doi:10.1016/j.conbuildmat.2013.02.056.

[8] R. Paolini, A. Zani, T. Poli, F. Antretter, M. Zinzi, Natural aging of cool walls: Impact on solar reflectance, sensitivity to thermal shocks and building energy needs, Energy Build. 153 (2017) 287–296. doi:10.1016/j.enbuild.2017.08.017.

[9] D. Soler, A. Salandin, J.C. Micó, Lowest thermal transmittance of an external wall under budget, material and thickness restrictions: An integer linear programming approach, Energy Build. 158 (2018) 222–233. doi:10.1016/j.enbuild.2017.09.078.

[10] International Organization for Standardization, ISO 9869-1:2014 - Thermal insulation - Building elements - In situ measurement of thermal resistance and thermal transmittance. Part 1: Heat flow meter method, Geneva, Switzerland, 2014.

[11] P.G. Cesaratto, M. De Carli, S. Marinetti, Effect of different parameters on the in situ thermal conductance evaluation, Energy Build. 43 (2011) 1792–1801. doi:10.1016/j.enbuild.2011.03.021.

[12] G. Desogus, S. Mura, R. Ricciu, Comparing different approaches to in situ measurement of building components thermal resistance, Energy Build. 43 (2011) 2613–2620. doi:10.1016/j.enbuild.2011.05.025.

[13] C. Peng, Z. Wu, In situ measuring and evaluating the thermal resistance of building construction, Energy Build. 40 (2008) 2076–2082. doi:10.1016/j.enbuild.2008.05.012.

[14] X. Meng, B. Yan, Y. Gao, J. Wang, W. Zhang, E. Long, Factors affecting the in situ measurement accuracy of the wall heat transfer coefficient using the heat flow meter method, Energy Build. 86 (2015) 754–765. doi:10.1016/j.enbuild.2014.11.005.

[15] P. Baker, U-values and traditional buildings: in situ measurements and their comparisons to calculated values, 2011.

[16] F.G.N. Li, A.Z.P. Smith, P. Biddulph, I.G. Hamilton, R. Lowe, A. Mavrogianni, E. Oikonomou, R. Raslan, S. Stamp, A. Stone, A.J. Summerfield, D. Veitch, V. Gori, T. Oreszczyn, Solid-wall U-values: heat flux measurements compared with standard assumptions, Build. Res. Inf. 43 (2014) 238–252. doi:10.1080/09613218.2014.967977.

[17] D. Bienvenido-Huertas, R. Rodríguez-Álvaro, J.J. Moyano, F. Rico, D. Marín, Determining the U-Value of Façades Using the Thermometric Method: Potentials and Limitations, Energies. 11 (2018) 1–17. doi:10.3390/en11020360.

[18] S.-H. Kim, J.-H. Kim, H.-G. Jeong, K.-D. Song, Reliability Field Test of the Air–Surface Temperature Ratio Method for In Situ Measurement of U-Values, Energies. 11 (2018) 1–15. doi:10.3390/en11040803.

[19] X. Meng, Y. Gao, Y. Wang, B. Yan, W. Zhang, E. Long, Feasibility experiment on the simple hot box-heat flow meter method and the optimization based on simulation reproduction, Appl. Therm. Eng. 83 (2015) 48–56. doi:10.1016/j.applthermaleng.2015.03.010.

[20] F. Asdrubali, G. Baldinelli, Thermal transmittance measurements with the hot box method: Calibration, experimental procedures, and uncertainty analyses of three different approaches, Energy Build. 43 (2011) 1618–1626. doi:10.1016/j.enbuild.2011.03.005.

[21] F. Chen, S.K. Wittkopf, Summer condition thermal transmittance measurement of fenestration systems using calorimetric hot box, Energy Build. 53 (2012) 47–56. doi:10.1016/J.ENBUILD.2012.07.005.

[22] L. Pan, B. Chen, Z. Fang, Y. Zhen, Field Measurement and Data Processing Method of Envelope's Thermal Resistance, Build. Energy Environ. 6 (2005) 80–84.

[23] L. Pan, B. Chen, Z. Fang, B. Han, Y. Zheng, T. Zhang, Measurement of Thermal Resistance of Building Enclosures by Means of the Hotbox-Heat Flow meter Method [J], Ind. Heat. 3 (2006) 13.

[24] X. Zhu, L. Li, X. Yin, S. Zhang, Y. Wang, W. Lui, L. Zheng, An In-situ Test Apparatus of Heat Transfer Coefficient for Building Envelope, Build. Energy Effic. 256 (2012) 57–60.

[25] R. Albatici, A.M. Tonelli, Infrared thermovision technique for the assessment of thermal transmittance value of opaque building elements on site, Energy Build. 42 (2010) 2177–2183. doi:10.1016/j.enbuild.2010.07.010.

[26] G. Dall'O', L. Sarto, A. Panza, Infrared screening of residential buildings for energy audit purposes: Results of a field test, Energies. 6 (2013) 3859–3878. doi:10.3390/en6083859.

[27] R. Albatici, A.M. Tonelli, M. Chiogna, A comprehensive experimental approach for the validation of quantitative infrared

thermography in the evaluation of building thermal transmittance, Appl. Energy. 141 (2015) 218–228. doi:10.1016/j.apenergy.2014.12.035.

[28] I. Nardi, D. Paoletti, D. Ambrosini, T. De Rubeis, S. Sfarra, U-value assessment by infrared thermography: A comparison of different calculation methods in a Guarded Hot Box, Energy Build. 122 (2016) 211–221. doi:10.1016/j.enbuild.2016.04.017.

[29] L. Evangelisti, C. Guattari, P. Gori, F. Bianchi, Heat transfer study of external convective and radiative coefficients for building applications, Energy Build. 151 (2017) 429–438. doi:10.1016/j.enbuild.2017.07.004.

[30] K. Watanabe, Architectural Planning Fundamentals, 1965.

[31] B. Lehmann, K. Ghazi Wakili, T. Frank, B. Vera Collado, C. Tanner, Effects of individual climatic parameters on the infrared thermography of buildings, Appl. Energy. 110 (2013) 29–43. doi:10.1016/j.apenergy.2013.03.066.

[32] S. Van De Vijver, M. Steeman, N. Van Den Bossche, K. Carbonez, A. Janssens, The influence of environmental parameters on the thermographic analysis of the building envelope, in: QIRT 2014 - 12th Int. Conf. Quant. InfraRed Thermogr., 2014.

[33] A. Hagishima, J. Tanimoto, K. Narita, Intercomparisons of Experimental Convective Heat Transfer Coefficients and Mass Transfer Coefficients of Urban Surfaces, Boundary-Layer Meteorol. 117 (2005) 551–576. doi:10.1007/s10546-005-2078-7.

[34] R.J. Cole, N.S. Sturrock, The convective heat exchange at the external surface of buildings, Build. Environ. 12 (1977) 207–214. doi:10.1016/0360-1323(77)90021-X.

[35] J.H. Watmuff, W.W.S. Charters, D. Proctor, Solar and wind induced external coefficients - Solar collectors, Coop. Mediterr. Pour l'Energie Solaire, Rev. Int. d'Heliotechnique. (1977) 56.

[36] J.A. Palyvos, A survey of wind convection coefficient correlations for building envelope energy systems' modeling, Appl. Therm. Eng. 28 (2008) 801–808. doi:10.1016/j.applthermaleng.2007.12.005.

[37] T. Defraeye, B. Blocken, J. Carmeliet, Convective heat transfer coefficients for exterior building surfaces: Existing correlations and CFD modelling, Energy Convers. Manag. 52 (2011) 512–522. doi:10.1016/j.enconman.2010.07.026.

[38] W. Nusselt, W. Jürges, Die Kuhlung einer ebenen Wand durch einen Luftstrom, Gesundheits Ing. 52 (1922) 641–642.

[39] W. Jürges, Der Wärmeübergang an einer ebenen Wand (heat transfer at a plane wall), Gesundh. Ing., Beiheft, 1924.

[40] W.H. McAdams, Heat transmission, McGraw-Hill, New York, 1954.

[41] M.G. Davies, Building heat transfer, John Wiley & Sons, 2004.

[42] H.H. Sogin, A Summary of Experiments on Local Heat Transfer From the Rear of Bluff Obstacles to a Low Speed Airstream, J. Heat Transfer. 86 (1964) 200–202. doi:10.1115/1.3687094.

[43] A. Schaak, Industrial Heat Transfer, Chapman & Hall, London, 1965.

[44] B.H. Jennings, Environmental engineering; analysis and practice, International Textbook Co, 1970.

[45] N.S. Sturrock, Localized Boundary-layer Heat Transfer from External Building Surfaces, University of Liverpool, 1971.

[46] J.W. Mitchell, Base Heat Transfer in Two-Dimensional Subsonic Fully Separated Flows, J. Heat Transfer. 93 (1971) 342–348. doi:10.1115/1.3449829.

[47] M. Lokmanhekim, Procedure for determining heating and cooling loads for computerized energy calculations. Algorithms for building heat transfer subroutines, ASHRAE, New York, 1971.

[48] N. Ito, Field experiment study on the convective heat transfer coefficient on exterior surface of a building, ASHRAE Trans. 78 (1972) 184–191.

[49] K. Kimura, Scientific basis of air conditioning, Applied Science Publishers, London, 1977.

[50] K. Nicol, The energy balance of an exterior window surface, Inuvik, N.W.T., Canada, Build. Environ. 12 (1977) 215–219. doi:10.1016/0360-1323(77)90022-1.

[51] P.J. Lunde, Solar thermal engineering : space heating and hot water systems, John Wiley & Sons, 1980.

[52] F.L. Test, R.C. Lessmann, A. Johary, Heat Transfer During Wind Flow over Rectangular Bodies in the Natural Environment, J. Heat Transfer. 103 (1981) 262–267. doi:10.1115/1.3244451.

[53] S. Sharples, Full-scale measurements of convective energy losses from exterior building surfaces, Build. Environ. 19 (1984) 31–39. doi:10.1016/0360-1323(84)90011-8.

[54] M. Yazdanian, J. Klems, Measurement of the Exterior Convective Film Coefficient for Windows in Low-Rise Buildings, ASHRAE

Trans. 100 (1993) 1–19.

[55] S.E.G. Jayamaha, N.E. Wijeysundera, S.K. Chou, Measurement of the heat transfer coefficient for walls, Build. Environ. 31 (1996) 399–407. doi:10.1016/0360-1323(96)00014-5.

[56] D.L. Loveday, A.H. Taki, Convective heat transfer coefficients at a plane surface on a full-scale building facade, Int. J. Heat Mass Transf. 39 (1996) 1729–1742. doi:10.1016/0017-9310(95)00268-5.

[57] A.H. Taki, D.L. Loveday, External convection coefficients for framed rectangular elements on building facades, Energy Build. 24 (1996) 147–154. doi:10.1016/0378-7788(96)00972-3.

[58] A. Hagishima, J. Tanimoto, Field measurements for estimating the convective heat transfer coefficient at building surfaces, Build. Environ. 38 (2003) 873–881. doi:10.1016/S0360-1323(03)00033-7.

[59] International Organization for Standardization, ISO 6946:2007 - Building components and building elements - Thermal resistance and thermal transmittance - Calculation method, Geneva, Switzerland, 2007.

[60] M. Mirsadeghi, D. Cóstola, B. Blocken, J.L.M. Hensen, Review of external convective heat transfer coefficient models in building energy simulation programs: Implementation and uncertainty, Appl. Therm. Eng. 56 (2013) 134–151. doi:10.1016/j.applthermaleng.2013.03.003.

[61] CIBSE, CIBSE Guide A: Environmental Design, 2015. doi:10.1016/0360-1323(94)00059-2.

[62] Y. Liu, D.J. Harris, Measurements of wind speed and convective coefficient on the external surface of a low-rise building, Int. J. Ambient Energy. 36 (2015) 225–234. doi:10.1080/01430750.2013.853204.

[63] J. Xie, Y. Cui, J. Liu, J. Wang, H. Zhang, Study on convective heat transfer coefficient on vertical external surface of island-reef building based on naphthalene sublimation method, Energy Build. 158 (2018) 300–309. doi:10.1016/j.enbuild.2017.09.092.

[64] J.F.C. Sham, T.Y. Lo, S.A. Memon, Verification and application of continuous surface temperature monitoring technique for investigation of nocturnal sensible heat release characteristics by building fabrics, Energy Build. 53 (2012) 108–116. doi:10.1016/j.enbuild.2012.06.018.

[65] B. Tejedor, M. Casals, M. Gangolells, X. Roca, Quantitative internal infrared thermography for determining in-situ thermal behaviour of façades, Energy Build. 151 (2017) 187–197. doi:10.1016/j.enbuild.2017.06.040.

[66] S.W. Churchill, H.H.S. Chu, Correlating equations for laminar and turbulent free convection from a horizontal cylinder, Int. J. Heat Mass Transf. 18 (1975) 1049–1053.

[67] J. Kim, J. Lee, J. Kim, C. Jang, H. Jeong, D. Song, Appropriate conditions for determining the temperature difference ratio via infrared camera, Build. Serv. Eng. Res. Technol. 37 (2015) 272–287. doi:10.1177/0143624415600701.

[68] K. Maroy, K. Carbonez, M. Steeman, N. Van Den Bossche, Assessing the thermal performance of insulating glass units with infrared thermography: Potential and limitations, Energy Build. 138 (2017) 175–192. doi:10.1016/j.enbuild.2016.10.054.

[69] J.F. Coronel Toro, L. Pérez-Lombard Martín de Oliva, Collection of tables, graphs and heat transfer equations, Department of Energy Engineering. University of Seville, 2013.

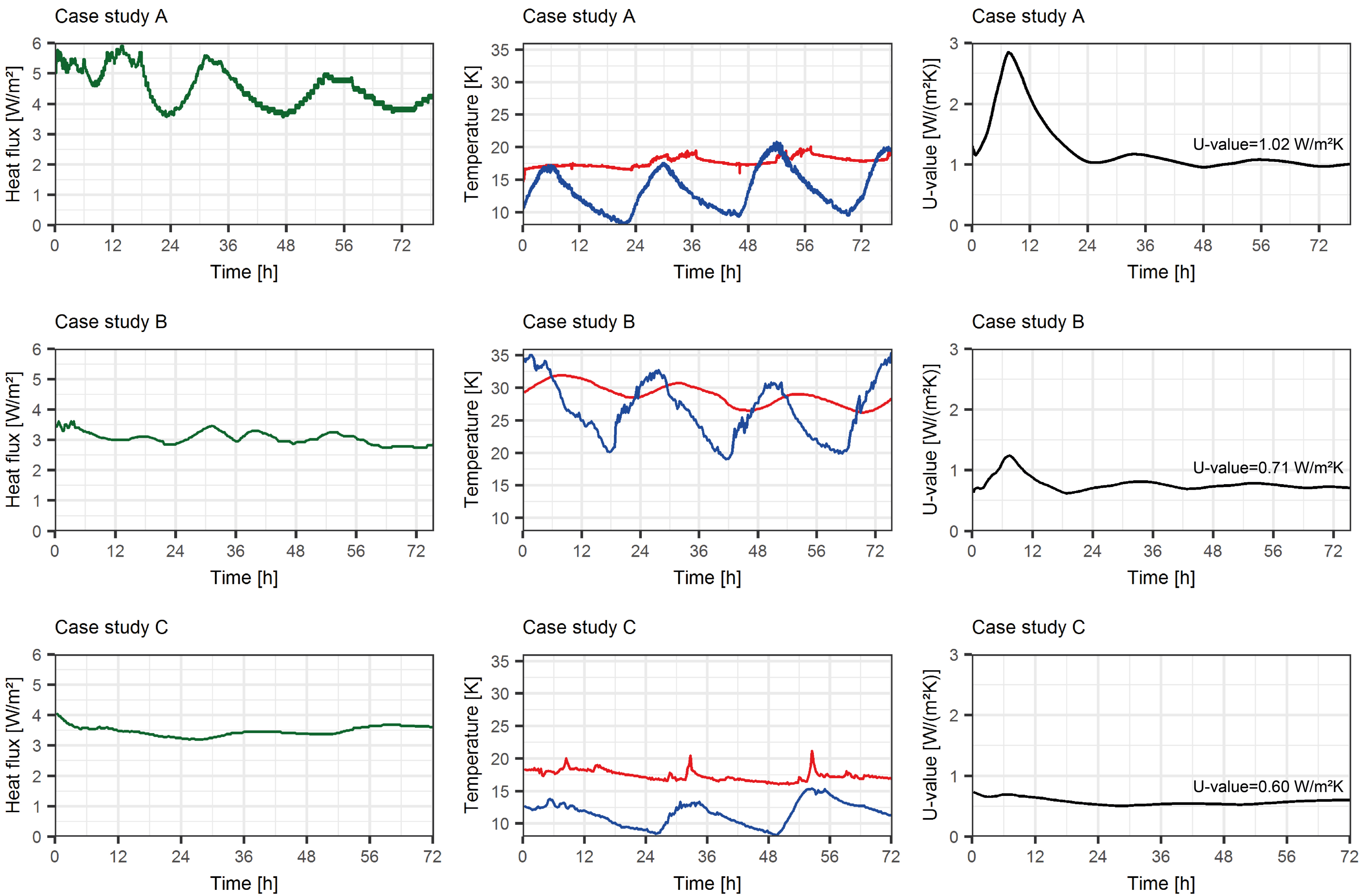
Case study A
Heat flux [W/m²]
Time [h]
Case study A
Temperature [K]
Time [h]
Case study A
U-value [W/(m²K)]
U-value=1.02 W/m²K
Time [h]
Case study B
Heat flux [W/m²]
Time [h]
Case study B
Temperature [K]
Time [h]
Case study B
U-value [W/(m²K)]
U-value=0.71 W/m²K
Time [h]
Case study C
Heat flux [W/m²]
Time [h]
Case study C
Temperature [K]
Time [h]
Case study C
U-value [W/(m²K)]
U-value=0.60 W/m²K
Time [h]

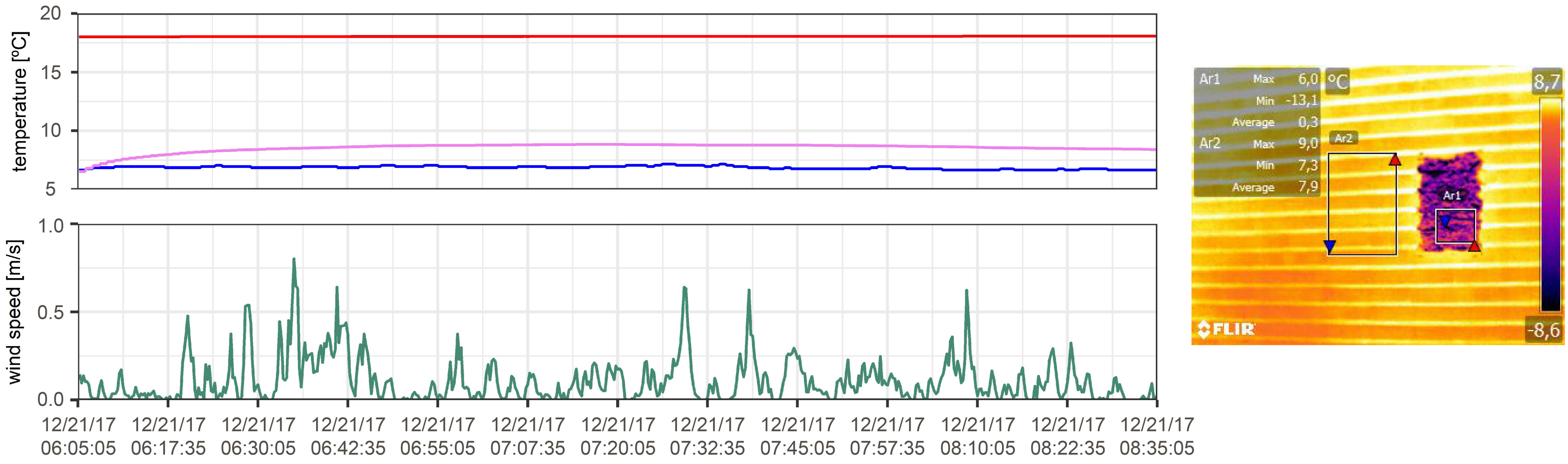

temperature [ºC]
20
15
10
5
wind speed [m/s]
1.0
0.5
0.0
12/21/17 06:05:05
12/21/17 06:17:35
12/21/17 06:30:05
12/21/17 06:42:35
12/21/17 06:55:05
12/21/17 07:07:35
12/21/17 07:20:05
12/21/17 07:32:35
12/21/17 07:45:05
12/21/17 07:57:35
12/21/17 08:10:05
12/21/17 08:22:35
12/21/17 08:35:05
Ar1 Max 6,0
Min -13,1
Average 0,3
Ar2 Max 9,0
Min 7,3
Average 7,9
°C
8,7
-8,6
Ar2
Ar1
FLIR

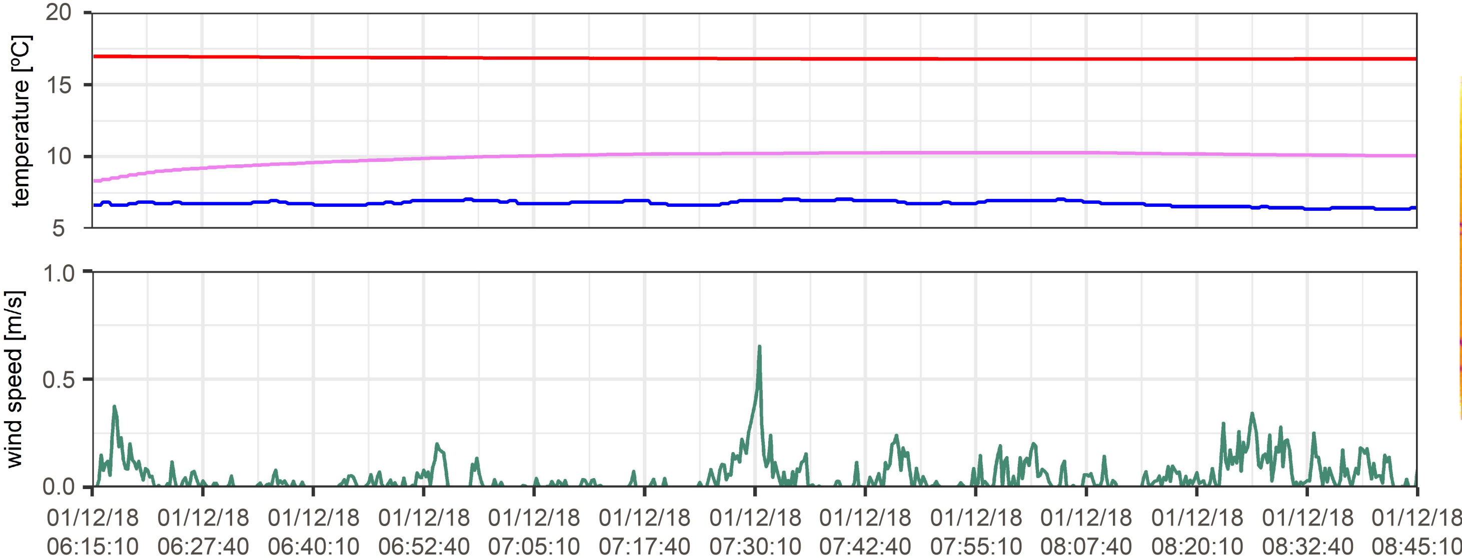
temperature [ºC]
20
15
10
5
wind speed [m/s]
1.0
0.5
0.0
01/12/18 06:15:10
01/12/18 06:27:40
01/12/18 06:40:10
01/12/18 06:52:40
01/12/18 07:05:10
01/12/18 07:17:40
01/12/18 07:30:10
01/12/18 07:42:40
01/12/18 07:55:10
01/12/18 08:07:40
01/12/18 08:20:10
01/12/18 08:32:40
01/12/18 08:45:10

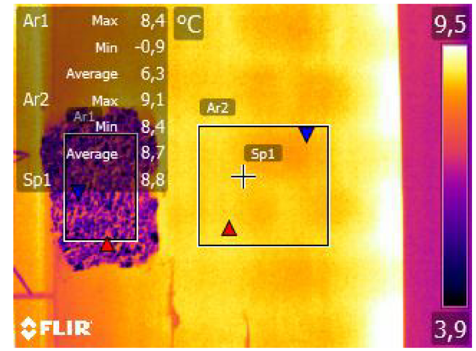
Ar1 Max 8,4
Min -0,9
Average 6,3
Ar2 Max 9,1
Min 8,4
Average 8,7
Sp1 8,8
°C
9,5
3,9
Ar1
Ar2
Sp1
FLIR

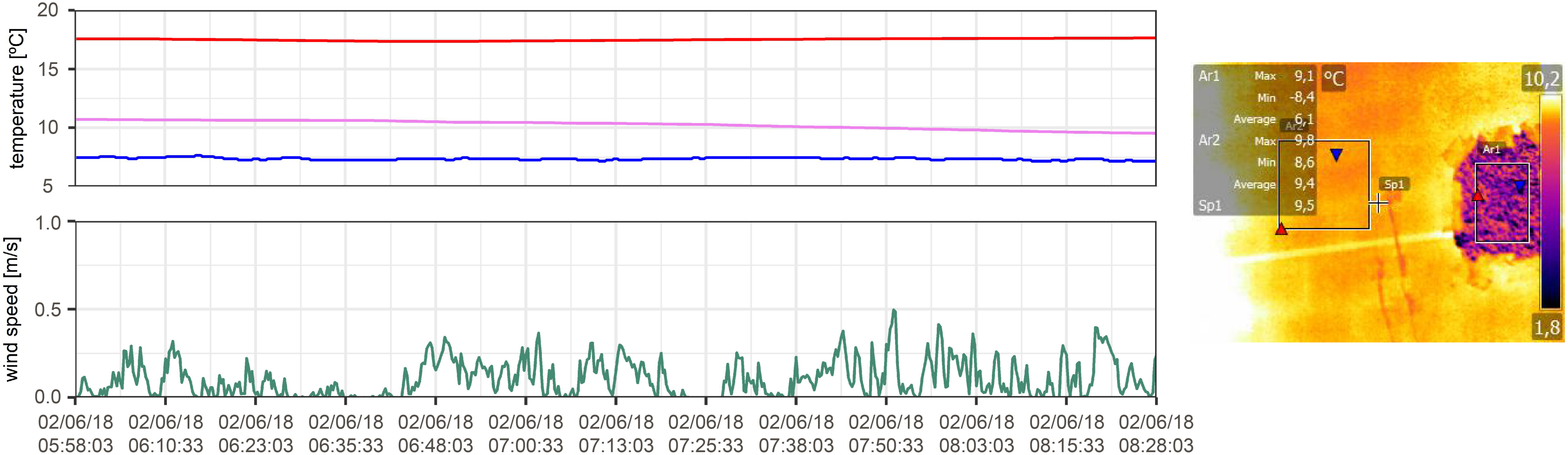

temperature [ºC]
20
15
10
5
wind speed [m/s]
1.0
0.5
0.0
02/06/18 05:58:03
02/06/18 06:10:33
02/06/18 06:23:03
02/06/18 06:35:33
02/06/18 06:48:03
02/06/18 07:00:33
02/06/18 07:13:03
02/06/18 07:25:33
02/06/18 07:38:03
02/06/18 07:50:33
02/06/18 08:03:03
02/06/18 08:15:33
02/06/18 08:28:03
Ar1 Max 9,1
Min -8,4
Average 6,1
Ar2 Max 9,8
Min 8,6
Average 9,4
Sp1 9,5
°C
10,2
1,8
Sp1
Ar1

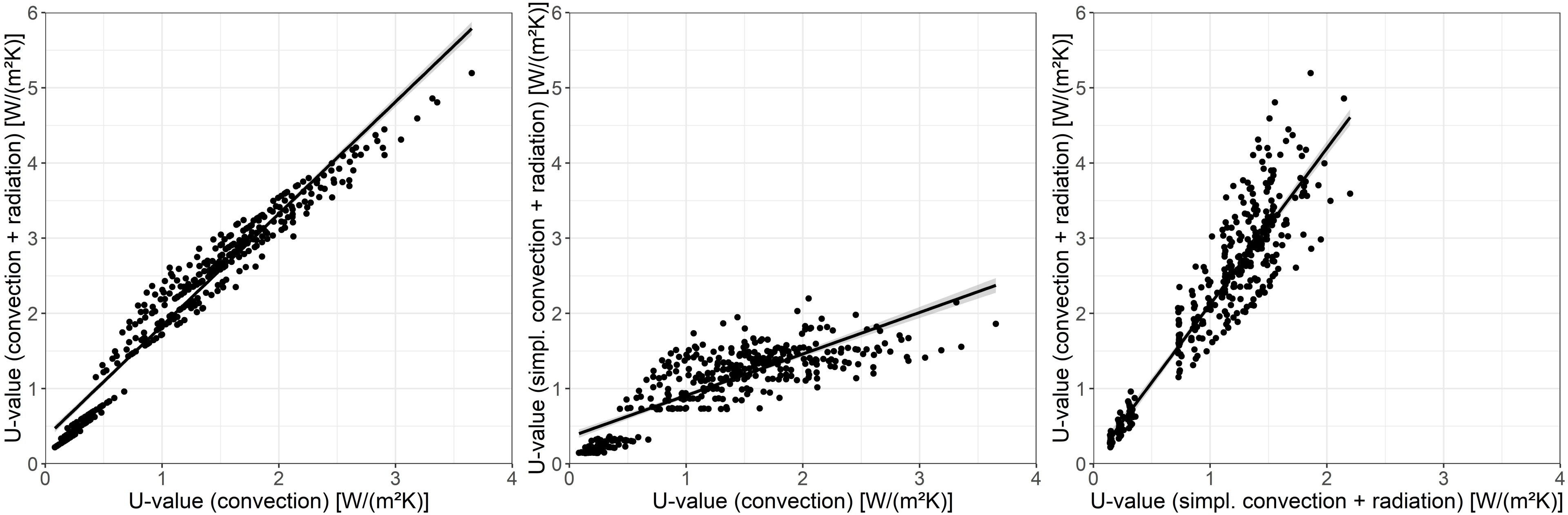
U-value (convection + radiation) [W/(m²K)]
U-value (convection) [W/(m²K)]
U-value (simpl. convection + radiation) [W/(m²K)]
U-value (convection) [W/(m²K)]
U-value (convection + radiation) [W/(m²K)]
U-value (simpl. convection + radiation) [W/(m²K)]

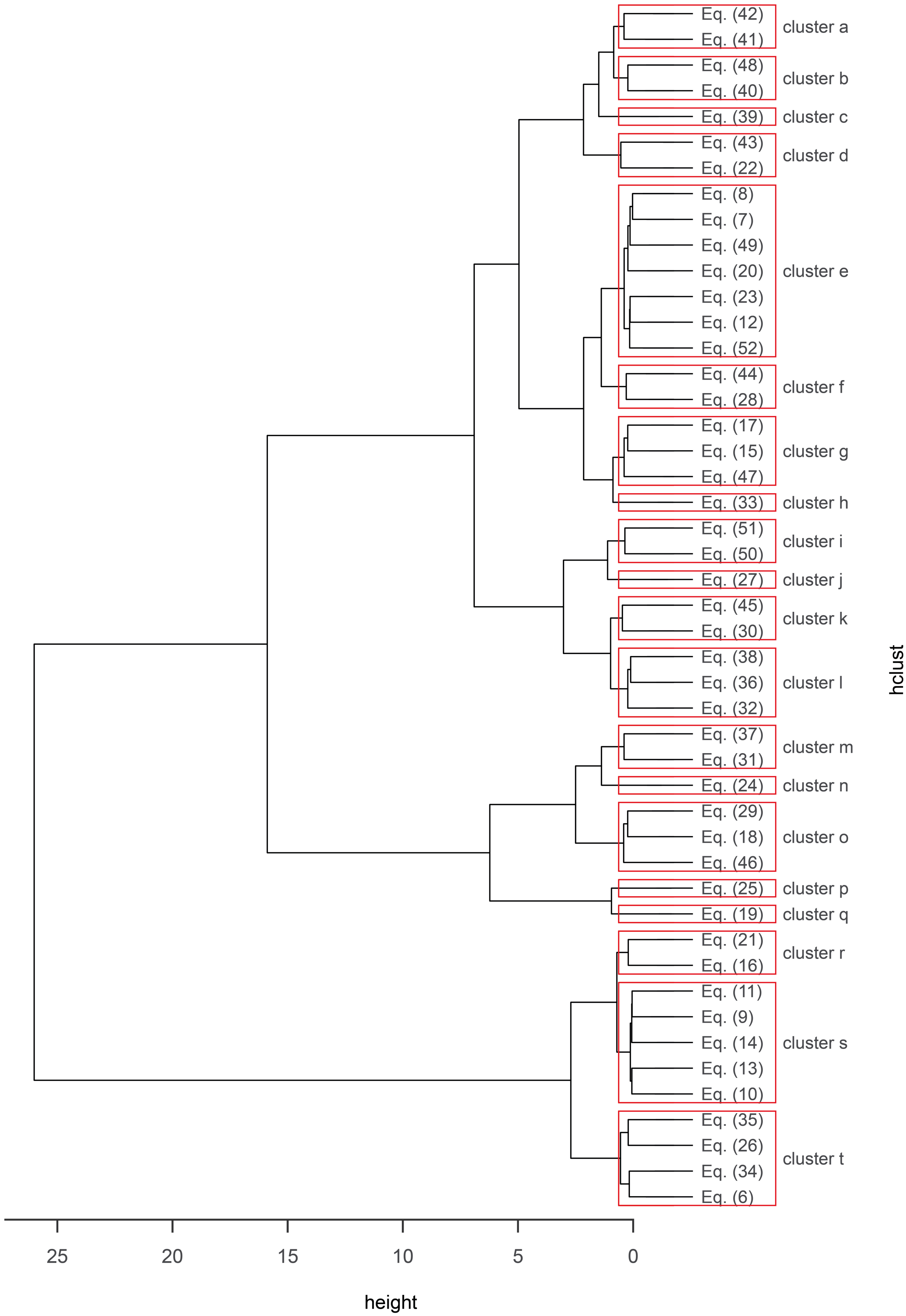
Eq. (42)
Eq. (41)
cluster a
Eq. (48)
Eq. (40)
cluster b
Eq. (39)
cluster c
Eq. (43)
Eq. (22)
cluster d
Eq. (8)
Eq. (7)
Eq. (49)
Eq. (20)
Eq. (23)
Eq. (12)
Eq. (52)
cluster e
Eq. (44)
Eq. (28)
cluster f
Eq. (17)
Eq. (15)
Eq. (47)
cluster g
Eq. (33)
cluster h
Eq. (51)
Eq. (50)
cluster i
Eq. (27)
cluster j
Eq. (45)
Eq. (30)
cluster k
Eq. (38)
Eq. (36)
Eq. (32)
cluster l
Eq. (37)
Eq. (31)
cluster m
Eq. (24)
cluster n
Eq. (29)
Eq. (18)
Eq. (46)
cluster o
Eq. (25)
cluster p
Eq. (19)
cluster q
Eq. (21)
Eq. (16)
cluster r
Eq. (11)
Eq. (9)
Eq. (14)
Eq. (13)
Eq. (10)
cluster s
Eq. (35)
Eq. (26)
Eq. (34)
Eq. (6)
cluster t
hclust
25
20
15
10
5
0
height

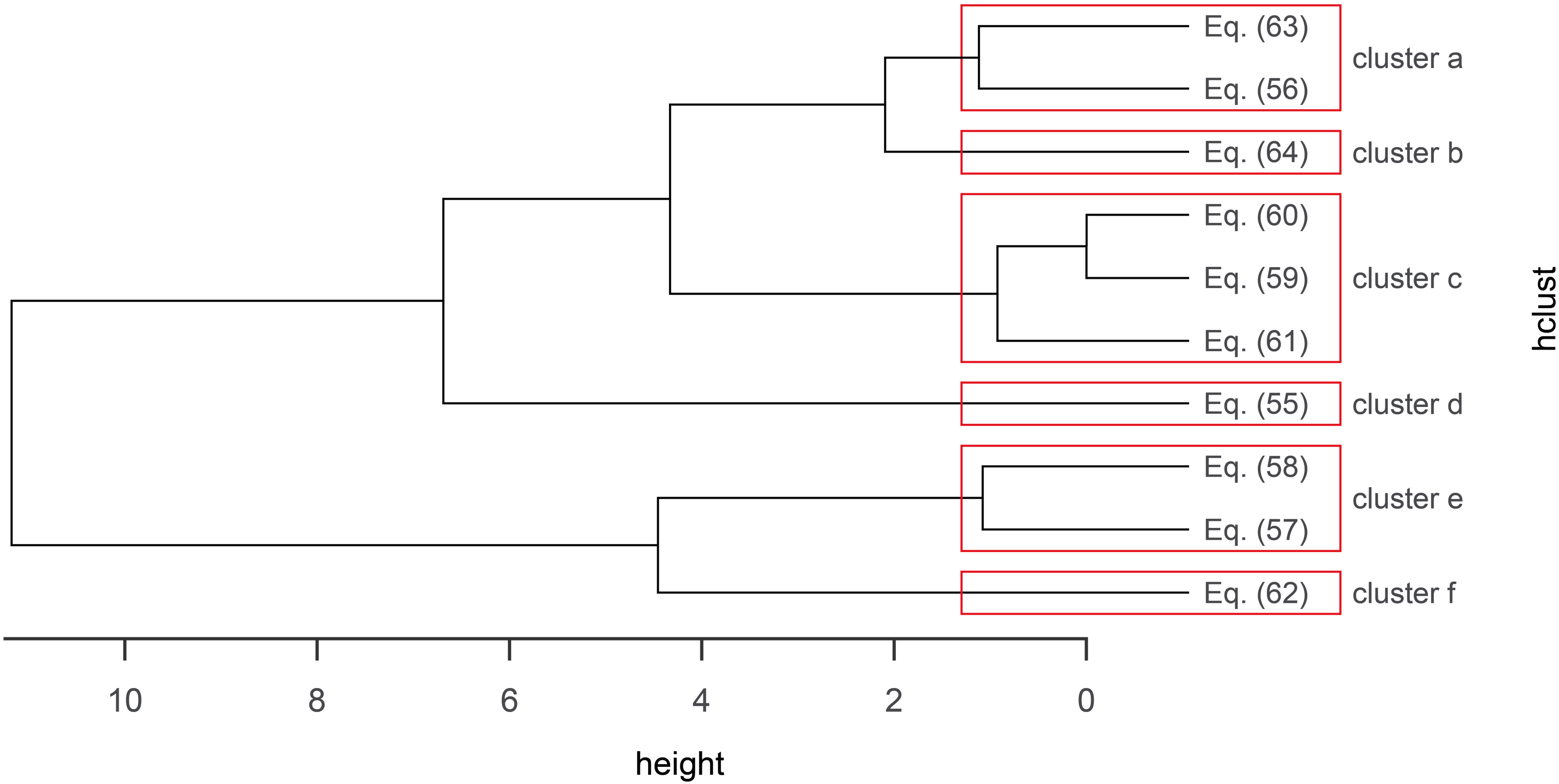

Eq. (63)
Eq. (56)
cluster a
Eq. (64)
cluster b
Eq. (60)
Eq. (59)
Eq. (61)
cluster c
Eq. (55)
cluster d
Eq. (58)
Eq. (57)
cluster e
Eq. (62)
cluster f
hclust
10
8
6
4
2
0
height

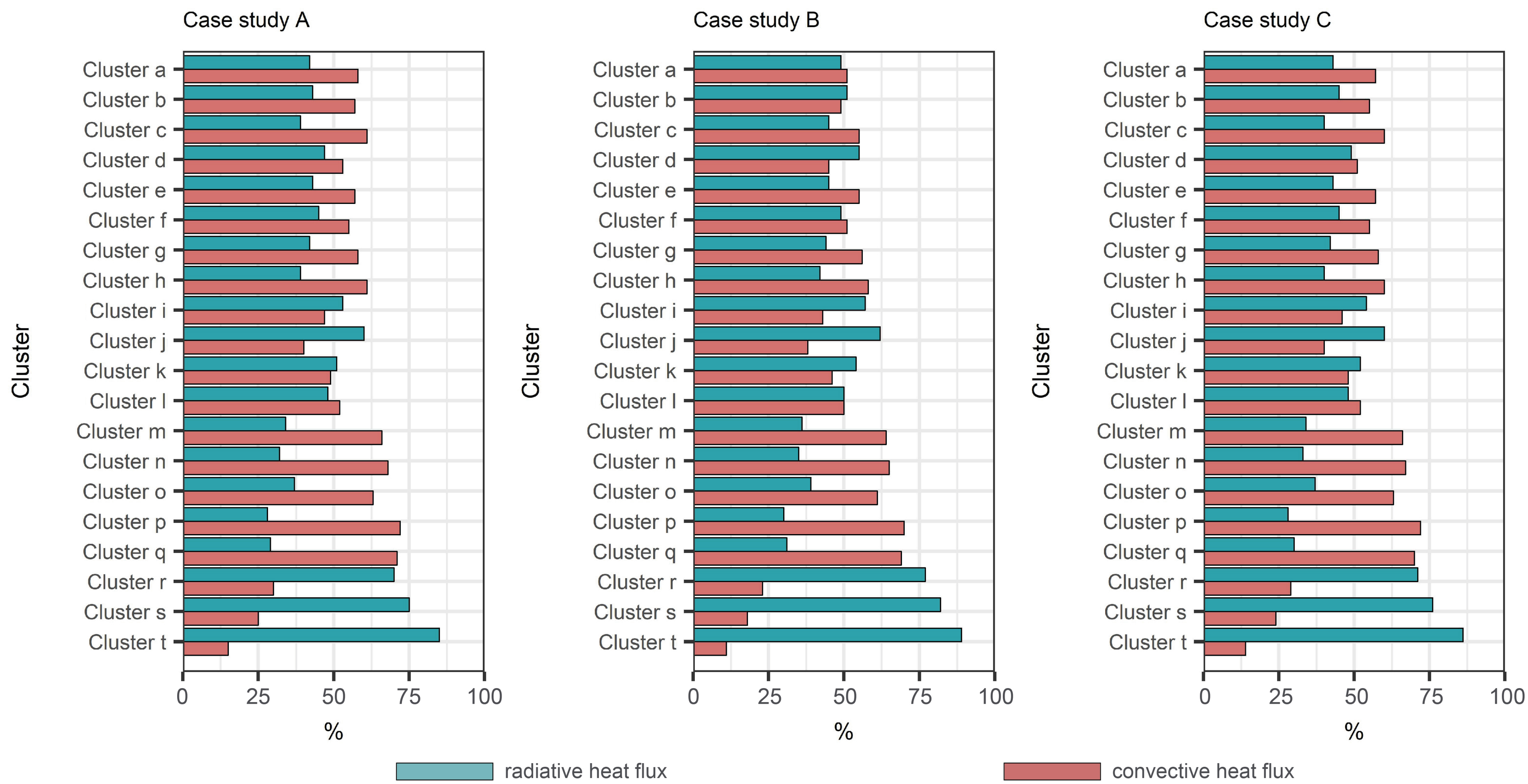

Case study A
Case study B
Case study C
Cluster
Cluster a
Cluster b
Cluster c
Cluster d
Cluster e
Cluster f
Cluster g
Cluster h
Cluster i
Cluster j
Cluster k
Cluster l
Cluster m
Cluster n
Cluster o
Cluster p
Cluster q
Cluster r
Cluster s
Cluster t
0
25
50
75
100
%
radiative heat flux
convective heat flux

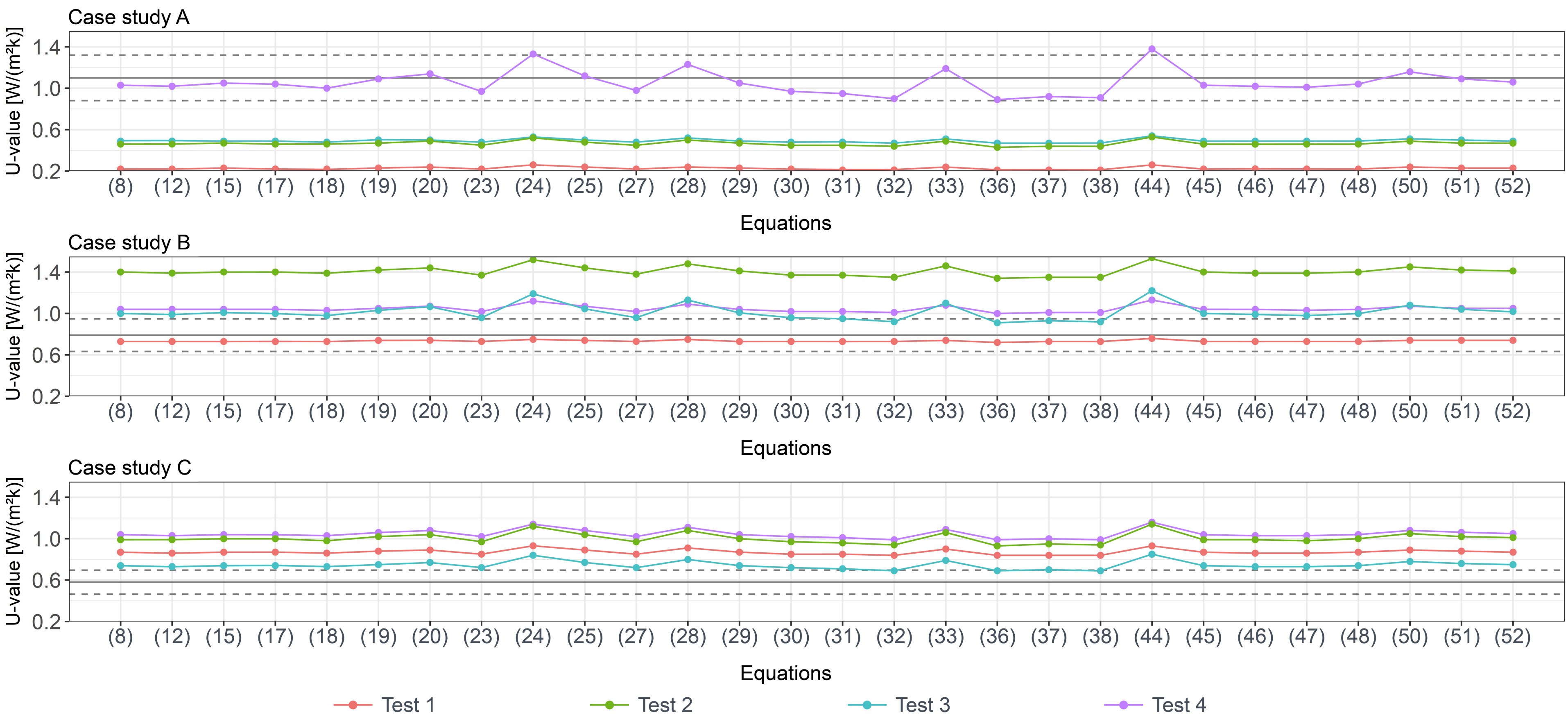

Case study A
Case study B
Case study C
U-value [W/(m²k)]
1.4
1.0
0.6
0.2
(8) (12) (15) (17) (18) (19) (20) (23) (24) (25) (27) (28) (29) (30) (31) (32) (33) (36) (37) (38) (44) (45) (46) (47) (48) (50) (51) (52)
Equations
Test 1
Test 2
Test 3
Test 4

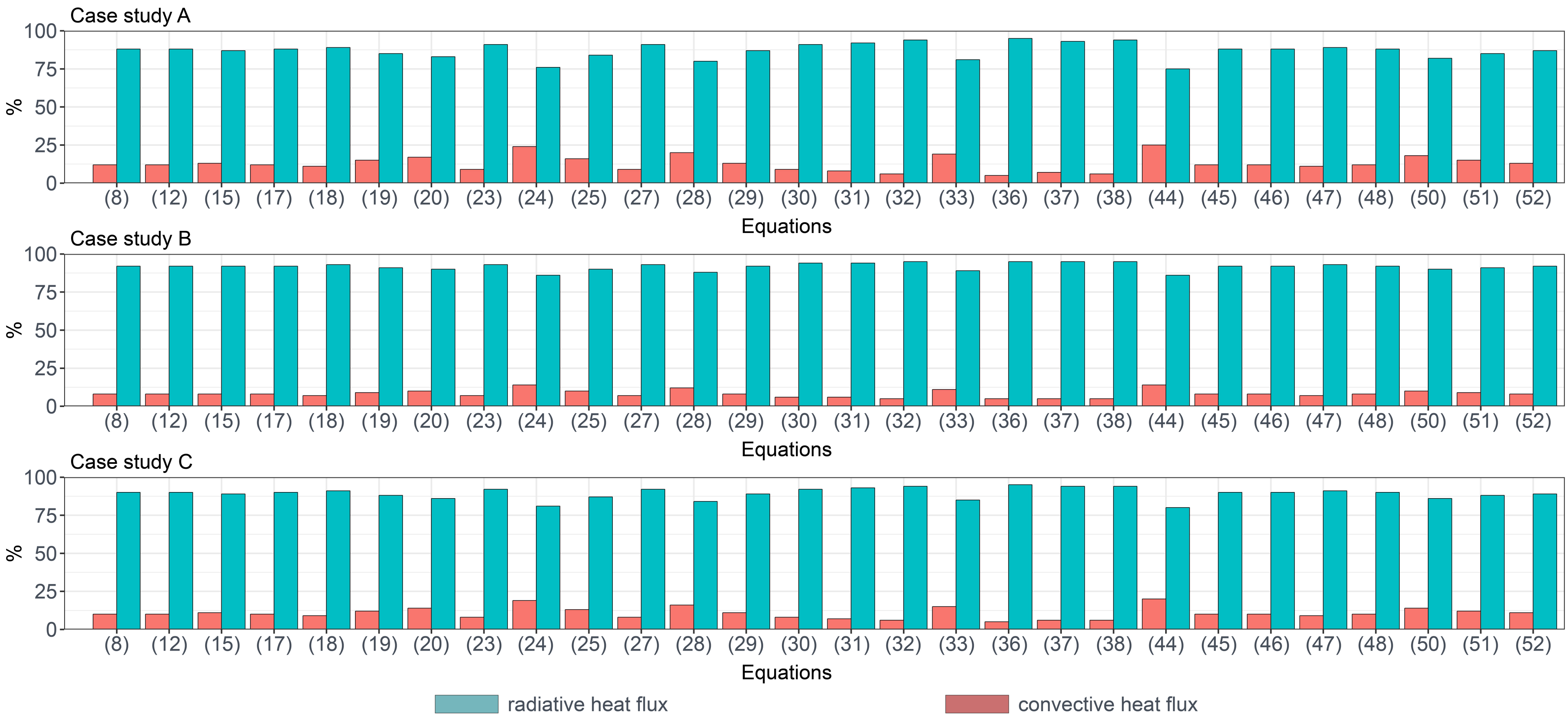

Case study A
Case study B
Case study C
%
100
75
50
25
0
(8) (12) (15) (17) (18) (19) (20) (23) (24) (25) (27) (28) (29) (30) (31) (32) (33) (36) (37) (38) (44) (45) (46) (47) (48) (50) (51) (52)
Equations
radiative heat flux
convective heat flux

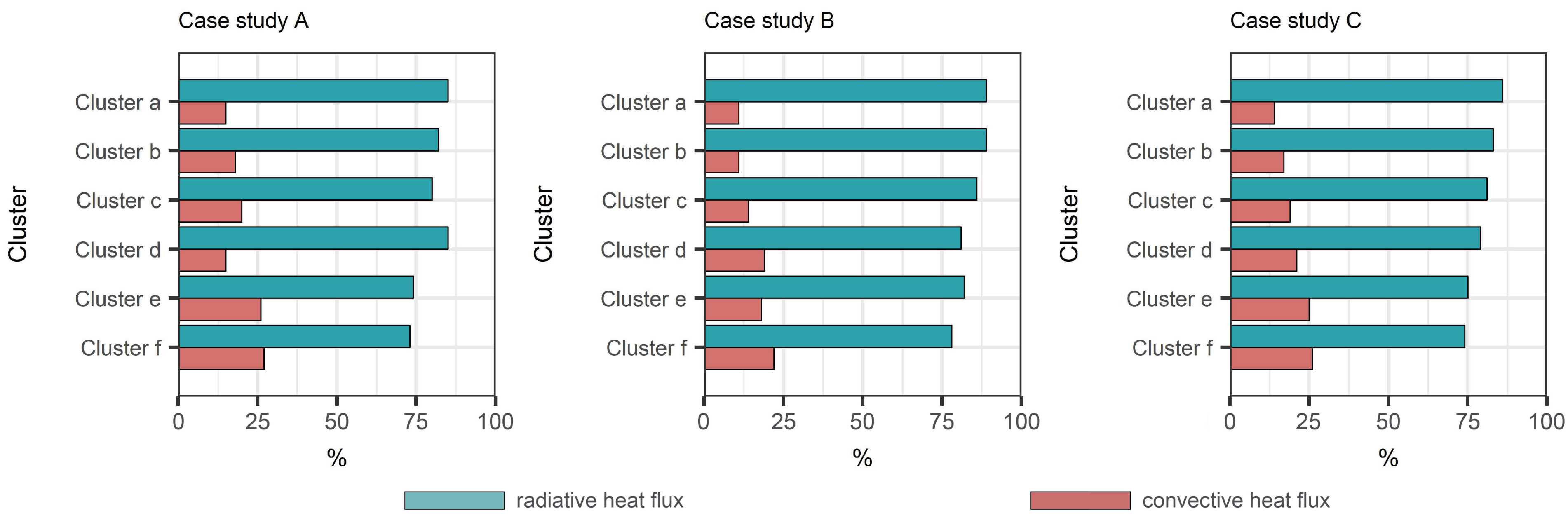
Case study A
Case study B
Case study C
Cluster
Cluster a
Cluster b
Cluster c
Cluster d
Cluster e
Cluster f
0
25
50
75
100
%
radiative heat flux
convective heat flux

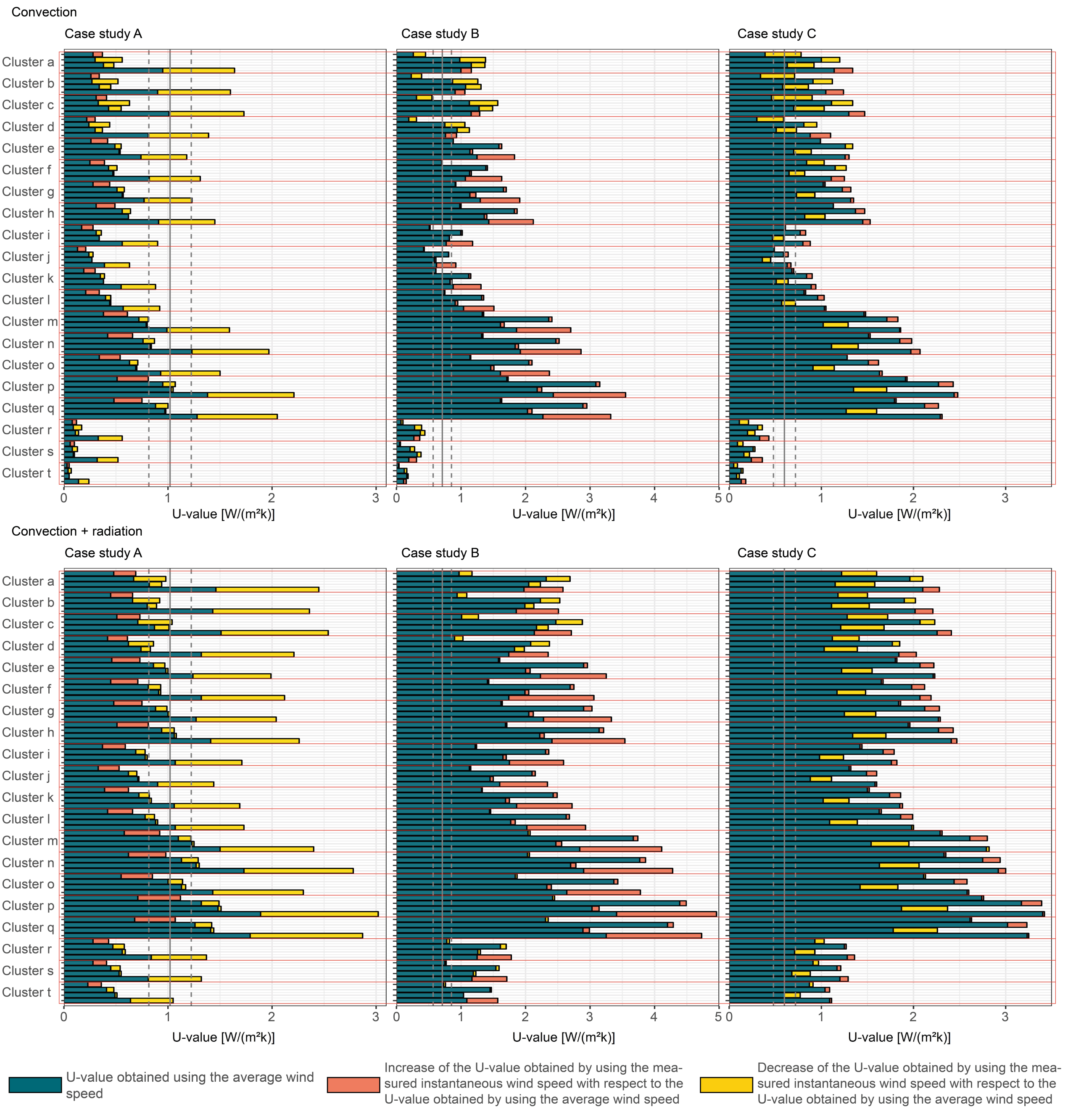
Convection
Case study A
Case study B
Case study C
Cluster a
Cluster b
Cluster c
Cluster d
Cluster e
Cluster f
Cluster g
Cluster h
Cluster i
Cluster j
Cluster k
Cluster l
Cluster m
Cluster n
Cluster o
Cluster p
Cluster q
Cluster r
Cluster s
Cluster t
0 1 2 3
0 1 2 3 4 5
0 1 2 3
U-value [W/(m²k)]
Convection + radiation
U-value obtained using the average wind speed
Increase of the U-value obtained by using the measured instantaneous wind speed with respect to the U-value obtained by using the average wind speed
Decrease of the U-value obtained by using the measured instantaneous wind speed with respect to the U-value obtained by using the average wind speed

Table 1
Approximations of ECHTC correlations of the wind speed.

ECHTC		Remarks	Reference
$h_e = 5.8 + 3.95v$	(8)	$v < 5$ m/s	Nusselt and Jürges [38]
$h_e = 7.13v^{0.78}$	(9)	$5 < v < 24$ m/s	Nusselt and Jürges [38]
$h_e = 7.11v^{0.775}$	(10)	Soft surfaces, $5 < v < 24$ m/s	Jürges [39]
$h_e = 7.52v^{0.784}$	(11)	Rough surfaces, $5 < v < 24$ m/s	Jürges [39]
$h_e = 5.7 + 3.8v$	(12)	Soft surfaces, $v < 5$ m/s	McAdams [40]
$h_e = 7.2v^{0.78}$	(13)	Soft surfaces, $v > 5$ m/s	McAdams [40]
$h_e = 7.6v^{0.78}$	(14)	Rough surfaces, $v > 5$ m/s	McAdams [40]
$h_e = 6.2 + 4.3v$	(15)	Rough surfaces, $v < 5$ m/s	Davies [41]
$h_e = 6.97v^{0.666}$	(16)	-	Sogin [42]
$h_e = 6.05 + 4.08v$	(17)	Rough surfaces, $v \leq 5$ m/s	Schaak [43]
$h_e = 7.82 + 3.50v$	(18)	Soft surfaces, without speed limit	Jennings [44]
$h_e = 10.7 + 4.96v$	(19)	Smooth brick, without speed limit	Jennings [44]
$h_e = 5.7 + 6v$	(20)	Heating	Sturrock [45]
$h_e = 6.60v^{0.6}$	(21)	-	Mitchell [46]
$h_e = 18.65v^{0.605}$	(22)	-	Lokmanhekim [47]
$h_e = 5.8 + 2.9v$	(23)	Windward, free stream wind speed superior a 3 m/s	Ito [48]
$h_e = 8.7 + 9.4v$	(24)	Leeward, $v > 4$ m/s	Ito [48]
$h_e = 11.4 + 5.7v$	(25)	Heating, normal surface, $v < 5$ m/s	Cole and Sturrock [34]
$h_e = 5.7v$	(26)	Heating, leeward surface, $v < 5$ m/s	Cole and Sturrock [34]
$h_e = 2.8 + 3.0v$	(27)	Correction of the ECHTC of Jürges (Eq. (8)), $v < 5$ m/s	Watmuff et al. [35]
$h_e = 4.7 + 7.6v$	(28)	-	Kimura [49]
$h_e = 7.55 + 4.35v$	(29)	-	Nicol [50]
$h_e = 4.5 + 2.9v$	(30)	Soft surfaces	Lunde [51]
$h_e = 8.55 + 2.56v$	(31)	-	Test et al. [52]
$h_e = 5.1 + 1.7v$	(32)	$0.5 < v < 20$ m/s	Sharples [53]
$h_e = 6.47 + 6.806v$	(33)	-	Yazdanian and Klems [54]
$h_e = 2.38v^{0.89}$	(34)	Forced convection, windward	Yazdanian and Klems [54]
$h_e = 2.86v^{0.617}$	(35)	Forced convection, leeward	Yazdanian and Klems [54]
$h_e = 4.955 + 1.444v$	(36)	-	Jayamaha et al. [55]
$h_e = 8.91 + 2.00v$	(37)	Windward	Loveday and Taki [56]
$h_e = 4.93 + 1.77v$	(38)	Leeward	Loveday and Taki [56]
$h_e = 16.15v^{0.397}$	(39)	Windward, $0.5 < v < 9$ m/s	Loveday and Taki [56]
$h_e = 16.25v^{0.503}$	(40)	Leeward, $0.5 < v < 9$ m/s	Loveday and Taki [56]
$h_e = 16.21v^{0.452}$	(41)	Correlation for windward and leeward	Loveday and Taki [56]
$h_e = 14.82v^{0.42}$	(42)	Windward, $0 < v < 10$ m/s	Taki and Loveday [57]
$h_e = 15.06v^{0.53}$	(43)	Leeward, $0 < v < 4.5$ m/s	Taki and Loveday [57]
$h_e = 4.47 + 10.21v$	(44)	$0.5 < v < 3$ m/s	Hagishima and Tanimoto [58]
$h_e = 4 + 4v$	(45)	-	ISO 6946 [59]
$h_e = 7.4 + 3.8v$	(46)	Rough surfaces, $v < 15$ m/s	Mirsadeghi et al. [60]
$h_e = 6.5 + 3.6v$	(47)	Soft surfaces, $v < 15$ m/s	Mirsadeghi et al. [60]
$h_e = 16.7v^{0.5}$	(48)	-	Mirsadeghi et al. [60]
$h_e = 5.8 + 4.1v$	(49)	-	CIBSE [61]
$h_e = 3.32 + 6.31v$	(50)	Windward, $0 < v < 3.5$ m/s	Liu and Harris [62]
$h_e = 3.19 + 5.03v$	(51)	Leeward, $0 < v < 3.5$ m/s	Liu and Harris [62]
$h_e = 5.56 + 4.48v$	(52)	Rough surfaces, $v < 5$ m/s	Xie et al. [63]

Table 2

Approximations of ECHTC correlations of dimensionless numbers.

ECHTC		Remarks	Reference
$h_e = \frac{k(0.10Re^{0.666})}{L}$	(56)	Windward	Nusselt and Jürges [38]
$h_e = \frac{k(0.20Re^{0.666})}{L}$	(57)	Leeward	Nusselt and Jürges [38]
$h_e = \frac{k(0.42Re^{0.6})}{L}$	(58)	-	Jürges [39]
$h_e = \frac{k(0.931Re^{0.5}Pr^{0.333})}{L}$	(59)	-	Jürges [39]
$h_e = \frac{k(0.93Re^{0.5}Pr^{0.333})}{L}$	(60)	-	McAdams [40]
$h_e = \frac{k(0.86Re^{0.5}Pr^{0.333})}{L}$	(61)	-	McAdams [40]
$h_e = \frac{k(0.0253Re^{0.8} + 3)}{L}$	(62)	-	McAdams [40]
$h_e = \frac{k(0.664Re^{0.5}Pr^{0.33})}{L}$	(63)	Laminar flow	Davies [41]
$h_e = \frac{k(0.037Re^{0.8}Pr^{0.33})}{L}$	(64)	Turbulent flow	Sogin [42]

Table 3
Technical characteristics and thermo-physical properties of case studies.

#	Case study A (1966)	s [mm]	λ [W/(m·K)]	R [(m²·K)/W]	Sketch
1	Perforated brick	115	0.35	-	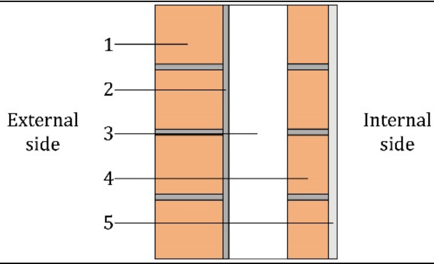
2	Cement mortar	10	1.30	-	
3	Air gap	100	-	0.18	
4	Hollow brick	70	0.32	-	
5	Gypsum plaster	15	0.57	-	
U = 1.10 [W/(m²·K)]					
#	Case study B (2005)	s [mm]	λ [W/(m·K)]	R [(m²·K)/W]	Sketch
1	Cement mortar	15	1.30	-	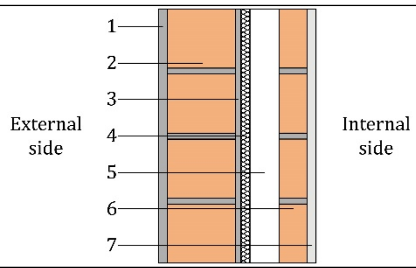
2	Perforated brick	115	0.35	-	
3	Cement mortar	10	1.30	-	
4	Insulation PUR	15	0,035	-	
5	Air gap	50	-	0.18	
6	Hollow brick	50	0.32	-	
7	Gypsum plaster	15	0.57	-	
U = 0.79 [W/(m²·K)]					
#	Case study C (2017)	s [mm]	λ [W/(m·K)]	R [(m²·K)/W]	Sketch
1	Cement mortar	15	1.30	-	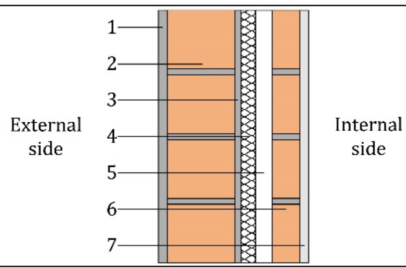
2	Perforated brick	117	0.35	-	
3	Cement mortar	10	1.30	-	
4	Insulation PUR	25	0,028	-	
5	Air gap	28	-	0.18	
6	Hollow brick	50	0.32	-	
7	Gypsum plaster	15	0.57	-	
U = 0.58 [W/(m²·K)]					

s: thickness; λ: thermal conductivity; R: thermal resistance.

Table 4
Main technical specifications of the equipment employed.

Equipment	Input	Measuring range	Resolution	Accuracy
Data logger ALMEMO 2590-4AS				
with thermocouples T 190-2	Temperature	-10 to 105 °C	0.1 K	±0.05 K ±0.05 %
	Wire diameter	0.5 mm		
Infrared camera FLIR E60bx	FOV	25°x19°		
	IFOV	1.36 mrad		
	Sensor	FPA, uncooled microbolometer		
	Spectral range	7.5-13 μm		
	Thermal sensitivity	<0.05-30 °C		
Hot-wire anemometer PCE-423	Wind speed	0-25 m/s	0.01 m/s	±5 %

Table 5

Statistical parameters of regressions of the different theoretical approaches.

Convection + radiation Convection		Convection (simpl.) + radiation Convection		Convection (simpl.) + radiation Convection + radiation	
R^2	*MAE*	R^2	*MAE*	R^2	*MAE*
0.94	0.97	0.66	0.34	0.85	1.18

Table 6

Thermal transmittance results obtained for ECHTC correlations depending on the wind speed for the approach which only uses the convective heat transfer coefficient.

Cluster	*U*-value [W/(m²·K)]											
	Case study A				Case study B				Case study C			
	Test 1	Test 2	Test 3	Test 4	Test 1	Test 2	Test 3	Test 4	Test 1	Test 2	Test 3	Test 4
a	0.28±0.11	0.56±0.06	0.49±0.10	1.64±0.32	0.45±0.03	1.38±0.13	1.37±0.37	1.00±0.04	0.78±0.13	1.20±0.13	0.92±0.12	1.14±0.09
b	0.26±0.10	0.53±0.06	0.45±0.10	1.60±0.31	0.39±0.03	1.26±0.12	1.31±0.35	0.91±0.04	**0.71±0.12**	1.12±0.12	0.86±0.11	1.05±0.09
c	0.31±0.12	0.63±0.07	0.56±0.12	1.73±0.34	0.55±0.04	1.57±0.15	1.49±0.41	1.16±0.05	0.90±0.15	1.34±0.15	1.02±0.13	1.30±0.11
d	0.22±0.08	0.44±0.05	0.38±0.08	1.39±0.27	0.31±0.03	1.06±0.10	1.13±0.28	**0.76±0.03**	**0.59±0.10**	0.95±0.10	0.73±0.09	0.88±0.07
e	0.27±0.10	0.56±0.06	0.54±0.12	**1.18±0.23**	0.89±0.07	1.59±0.15	1.14±0.29	1.25±0.05	0.99±0.16	1.34±0.13	0.89±0.12	1.26±0.10
f	0.25±0.09	0.51±0.06	0.48±0.10	1.31±0.26	**0.71±0.05**	1.38±0.13	1.14±0.29	1.06±0.05	0.84±0.14	1.06±0.11	0.82±0.10	1.16±0.09
g	0.28±0.11	0.58±0.07	0.57±0.15	**1.23±0.25**	0.93±0.07	1.66±0.16	1.19±0.31	1.30±0.06	1.03±0.17	1.26±0.14	0.93±0.12	1.32±0.11
h	0.31±0.12	0.65±0.07	0.63±0.13	1.45±0.28	1.00±0.07	1.83±0.18	1.36±0.36	1.43±0.06	1.13±0.19	1.37±0.15	1.04±0.13	1.45±0.12
i	0.17±0.07	0.36±0.04	0.34±0.07	**0.90±0.18**	0.52±0.04	1.00±0.09	**0.80±0.17**	**0.77±0.03**	**0.61±0.10**	0.77±0.08	**0.58±0.07**	0.80±0.06
j	0.13±0.05	0.28±0.03	0.27±0.06	0.63±0.12	0.43±0.03	**0.79±0.07**	**0.59±0.10**	**0.63±0.02**	**0.49±0.08**	**0.59±0.06**	0.46±0.06	**0.63±0.05**
k	0.19±0.07	0.40±0.04	0.39±0.08	**0.89±0.17**	**0.61±0.05**	1.12±0.11	**0.83±0.18**	**0.88±0.04**	**0.69±0.11**	0.84±0.09	**0.64±0.08**	0.89±0.07
l	0.21±0.08	0.45±0.05	0.45±0.10	**0.91±0.18**	**0.75±0.06**	1.32±0.13	0.91±0.21	1.04±0.04	0.82±0.14	0.96±0.10	**0.72±0.09**	1.04±0.08
m	0.39±0.15	0.81±0.09	0.80±0.17	1.60±0.32	1.35±0.11	2.36±0.23	1.61±0.45	1.86±0.08	1.47±0.25	1.71±0.19	1.29±0.17	1.86±0.15
n	0.42±0.16	**0.87±0.10**	**0.84±0.18**	1.97±0.39	1.35±0.10	2.47±0.24	1.84±0.53	1.92±0.09	1.52±0.26	1.85±0.20	1.40±0.18	1.96±0.16
o	0.34±0.13	0.72±0.08	0.70±0.15	1.50±0.29	1.15±0.09	2.05±0.20	1.46±0.40	1.61±0.07	1.28±0.21	1.51±0.16	1.14±0.15	1.63±0.13
p	0.51±0.19	**1.07±0.12**	**1.05±0.22**	2.22±0.44	1.73±0.13	3.09±0.30	2.18±0.64	2.43±0.11	1.92±0.32	2.27±0.25	1.71±0.22	2.44±0.20
q	0.48±0.18	**1.00±0.12**	**0.99±0.21**	2.05±0.41	1.63±0.13	2.89±0.28	2.03±0.59	2.27±0.10	1.80±0.30	2.12±0.23	1.60±0.21	2.29±0.19
r	0.09±0.03	0.17±0.02	0.14±0.03	0.57±0.11	0.11±0.01	0.39±0.04	0.44±0.09	0.27±0.01	0.21±0.03	0.36±0.04	0.28±0.03	0.33±0.02
s	0.07±0.03	0.13±0.01	0.10±0.02	0.53±0.10	0.06±0.01	0.28±0.03	0.37±0.08	0.19±0.01	0.14±0.02	0.28±0.03	0.21±0.03	0.24±0.02
t	0.04±0.01	0.07±0.01	0.05±0.01	0.24±0.05	0.04±0.01	0.16±0.01	0.18±0.05	0.11±0.01	0.08±0.01	0.15±0.01	0.11±0.01	0.13±0.01

Table 7

Thermal transmittance results obtained for ECHTC correlations depending on the wind speed for the approach which uses the convective and radiative component.

Cluster	*U*-value [W/(m²·K)]											
	Case study A				Case study B				Case study C			
	Test 1	Test 2	Test 3	Test 4	Test 1	Test 2	Test 3	Test 4	Test 1	Test 2	Test 3	Test 4
a	0.48±0.18	**0.98±0.11**	**0.95±0.20**	2.45±0.43	1.17±0.09	2.69±0.27	2.23±0.57	1.99±0.26	1.61±0.27	2.10±0.23	1.58±0.31	2.11±0.38
b	0.46±0.18	**0.94±0.11**	**0.91±0.19**	2.41±0.41	1.11±0.09	2.58±0.25	2.17±0.55	1.89±0.43	1.53±0.26	2.02±0.23	1.52±0.28	2.02±0.35
c	0.51±0.20	**1.05±0.12**	**1.01±0.22**	2.55±0.48	1.27±0.10	2.89±0.28	2.35±0.61	2.14±0.31	1.73±0.30	2.24±0.25	1.69±0.36	2.26±0.42
d	0.42±0.16	**0.86±0.10**	**0.83±0.18**	2.21±0.41	1.03±0.08	2.37±0.23	1.99±0.49	1.74±0.18	1.41±0.24	1.85±0.21	1.39±0.21	1.85±0.31
e	0.47±0.18	**0.98±0.11**	**1.00±0.21**	2.00±0.40	1.61±0.13	2.90±0.29	2.00±0.49	2.23±0.34	1.81±0.31	2.08±0.23	1.55±0.29	2.23±0.41
f	0.45±0.17	**0.93±0.11**	**0.93±0.20**	2.12±0.47	1.43±0.11	2.69±0.27	2.00±0.49	2.05±0.28	1.66±0.28	1.98±0.22	1.49±0.26	2.07±0.37
g	0.48±0.18	**1.00±0.12**	**1.02±0.22**	2.05±0.43	1.65±0.13	2.97±0.29	2.05±0.51	2.29±0.35	1.85±0.32	2.13±0.24	1.59±0.31	2.28±0.43
h	0.51±0.20	**1.07±0.12**	**1.08±0.23**	2.27±0.44	1.72±0.14	3.14±0.31	2.22±0.57	2.41±0.39	1.95±0.33	2.27±0.25	1.70±0.35	2.42±0.46
i	0.38±0.14	0.78±0.09	0.80±0.17	1.71±0.36	1.24±0.10	2.31±0.23	1.66±0.47	1.76±0.18	1.43±0.24	1.67±0.19	1.25±0.14	1.76±0.29
j	0.34±0.13	0.70±0.08	0.73±0.16	1.44±0.33	1.15±0.09	2.10±0.21	1.45±0.30	1.60±0.13	1.31±0.22	1.49±0.17	1.11±0.07	1.59±0.24
k	0.39±0.15	**0.82±0.09**	**0.84±0.18**	1.70±0.35	1.34±0.11	2.44±0.24	1.69±0.38	1.86±0.22	1.52±0.26	1.74±0.19	1.30±0.16	1.86±0.31
l	0.42±0.16	**0.87±0.10**	**0.91±0.19**	1.72±0.36	1.47±0.12	2.63±0.26	1.77±0.41	2.02±0.27	1.65±0.28	1.86±0.21	1.39±0.21	2.00±0.35
m	0.59±0.22	1.23±0.14	1.26±0.27	2.41±0.41	2.07±0.16	3.67±0.36	2.47±0.65	2.84±0.54	2.29±0.39	2.62±0.29	1.96±0.45	2.82±0.57
n	0.62±0.24	1.29±0.15	1.30±0.28	2.78±0.50	2.06±0.16	3.77±0.37	2.70±0.73	2.90±0.56	2.34±0.40	2.75±0.31	2.06±0.50	2.92±0.58
o	0.55±0.21	**1.14±0.13**	**1.17±0.25**	2.30±0.46	1.87±0.15	3.37±0.33	2.32±0.60	2.60±0.46	2.10±0.36	2.42±0.27	1.81±0.42	2.59±0.51
p	0.71±0.27	1.49±0.17	1.51±0.32	3.02±0.62	2.45±0.19	4.39±0.43	3.03±0.85	3.41±0.72	2.74±0.47	3.17±0.35	2.37±0.65	3.40±0.73
q	0.68±0.26	1.42±0.16	1.44±0.31	2.87±0.54	2.35±0.19	4.20±0.41	2.89±0.79	3.25±0.67	2.62±0.45	3.02±0.34	2.26±0.61	3.24±0.69
r	0.29±0.11	0.59±0.07	0.60±0.13	1.38±0.39	**0.83±0.07**	1.70±0.17	1.30±0.25	1.26±0.12	1.04±0.18	1.26±0.14	0.93±0.18	1.28±0.16
s	0.28±0.10	0.54±0.06	0.55±0.12	1.32±0.37	**0.77±0.06**	1.59±0.16	1.23±0.23	1.17±0.19	0.97±0.17	1.17±0.13	0.88±0.15	1.20±0.13
t	0.24±0.09	0.49±0.06	0.51±0.11	**1.05±0.33**	**0.76±0.06**	1.47±0.14	1.04±0.16	1.09±0.11	0.91±0.16	1.04±0.12	0.77±0.10	1.09±0.10

Table 8
Thermal transmittance results obtained for ECHTC correlations of dimensionless numbers for the approach which only uses the convective component.

Cluster	*U*-value [W/(m²·K)]											
	Case study A				Case study B				Case study C			
	Test 1	Test 2	Test 3	Test 4	Test 1	Test 2	Test 3	Test 4	Test 1	Test 2	Test 3	Test 4
a	0.04±0.01	0.07±0.01	0.06±0.01	0.21±0.05	0.05±0.01	0.16±0.02	0.16±0.06	0.11±0.04	0.10±0.02	0.15±0.02	0.12±0.01	0.14±0.01
b	0.04±0.02	0.08±0.01	0.06±0.01	0.34±0.07	0.03±0.01	0.16±0.02	0.21±0.07	0.11±0.04	0.09±0.02	0.18±0.02	0.14±0.01	0.16±0.01
c	0.05±0.02	0.10±0.01	0.08±0.02	0.30±0.06	0.07±0.01	0.22±0.02	0.23±0.08	0.16±0.05	0.13±0.02	0.21±0.02	0.16±0.01	0.20±0.01
d	0.03±0.02	0.07±0.02	0.05±0.01	0.17±0.05	0.06±0.01	0.31±0.04	0.23±0.08	0.30±0.09	0.40±0.09	0.23±0.03	0.20±0.01	0.29±0.02
e	0.07±0.03	0.13±0.01	0.10±0.02	0.46±0.07	0.06±0.01	0.26±0.03	0.31±0.11	0.18±0.06	0.16±0.03	0.27±0.03	0.21±0.02	0.25±0.02
f	0.08±0.03	0.15±0.02	0.14±0.03	0.42±0.06	0.18±0.01	0.38±0.04	0.33±0.11	0.29±0.09	0.23±0.04	0.32±0.04	0.25±0.02	0.32±0.02

Table 9
Thermal transmittance results obtained for ECHTC correlations of dimensionless numbers for the approach which uses the convective and radiative component.

Cluster	*U*-value [W/(m²·K)]											
	Case study A				Case study B				Case study C			
	Test 1	Test 2	Test 3	Test 4	Test 1	Test 2	Test 3	Test 4	Test 1	Test 2	Test 3	Test 4
a	0.23±0.09	0.49±0.06	0.52±0.11	**1.03±0.32**	**0.77±0.06**	1.47±0.14	1.02±0.16	1.09±0.36	0.92±0.16	1.05±0.12	0.78±0.10	1.10±0.11
b	0.24±0.09	0.50±0.06	0.52±0.11	**1.15±0.38**	**0.75±0.06**	1.47±0.14	1.07±0.17	1.09±0.36	0.92±0.16	1.08±0.12	0.80±0.11	1.11±0.11
c	0.25±0.10	0.52±0.06	0.54±0.12	**1.11±0.36**	**0.79±0.06**	1.53±0.15	1.08±0.17	1.14±0.38	0.95±0.16	1.11±0.12	0.82±0.12	1.16±0.12
d	0.23±0.09	0.49±0.05	0.50±0.10	**0.98±0.30**	**0.78±0.06**	1.62±0.17	1.09±0.18	1.28±0.42	1.22±0.23	1.13±0.13	0.86±0.14	1.24±0.15
e	0.27±0.10	0.56±0.06	0.57±0.12	1.27±0.39	**0.80±0.06**	1.60±0.16	1.18±0.21	1.18±0.39	0.99±0.17	1.19±0.13	0.89±0.15	1.23±0.14
f	0.27±0.11	0.57±0.07	0.59±0.13	1.23±0.38	0.89±0.07	1.69±0.17	1.19±0.21	1.27±0.42	1.06±0.18	1.22±0.14	0.91±0.16	1.28±0.15